PSERC

Automated Operating Procedures for Transfer Limits

Final Project Report

Power Systems Engineering Research Center

A National Science Foundation
Industry/University Cooperative Research Center
since 1996

Cornell • Arizona State • Berkeley • Carnegie Mellon • Colorado School of Mines
Georgia Tech • Illinois • Iowa State • Texas A&M • Washington State • Wisconsin

Automated Operating Procedures for Transfer Limits

Final Report

Research Team Faculty

Anjan Bose and Kevin Tomsovic (Project Leader)
Washington State University

Industry Representatives

Robert Stuart, Ben Williams and Mark Willis*
Pacific Gas and Electric

Research Team Students

Liqiang Chen and Mohammad Vaziri*
Washington State University

PSERC Publication 01-05

May 2001

*Presently with the California Independent System Operator

Information about this Project

For information about this project contact:

Kevin Tomsovic, Project Leader
Professor
School of Electrical Engineering and Computer Science
Washington State University
P.O. Box 642752
Pullman, WA 99164
Phone: 509-335-8260
Fax: 509-335-3818
Email: tomsovic@eecs.wsu.edu

Additional Copies of the Report

Copies of this report can be obtained from the Power Systems Engineering Research Center's website, www.pserc.wisc.edu. The PSERC publication number is 01-05. For additional information, contact:

Power Systems Engineering Research Center
Cornell University
428 Phillips Hall
Ithaca, New York 14853
Phone: 607-255-5601
Fax: 607-255-8871

Notice Concerning Copyright Material

Acknowledgements

The work described in this report was sponsored by the Power Systems Engineering Research Center (PSERC). We express our appreciation for the support provided by PSERC's industrial members and by the National Science Foundation through the following grant received under the Industry/University Cooperative Research Center program: NSF EEC 9813407 to Washington State University.

Executive Summary

A Modern Energy Management System (EMS) provides sophisticated online security analysis applications to assist operators in ensuring that the power system can survive credible contingencies. Still in current practice, system operators generally refer to written operating procedures to establish system constraints, particularly in regards to transfer limits across major interties. The limits are based on numerous power system studies that represent the stressed system and satisfy specific performance criteria following select contingencies. The relations between these critical paths and operating conditions are tabulated and often plotted as nomograms. With such a simplified view of system conditions, the operator is unable to have a complete understanding of operational limits. Thus, transfer ratings are typically conservative, as studies are based on highly stressed system conditions, and incomplete, as studies cannot analyze all combinations of equipment out-of-service. This study investigates some approaches to improving such operator procedures.

Ensuring system security usually means operating so as to maintain a specified margin, for example, real power reserve within a particular area. The required margins are generally mandated by the regional reliability organizations. Unfortunately, it is time-consuming to compute such limits and thus, the margins are primarily determined off-line. The operators then use the conservatively tabulated values to operate the system within limits. Ideally, as the system operating conditions change, the margins would be recomputed to precisely verify security. Since this is computationally infeasible, an alternative approach is to employ pattern matching methods. That is, by using the detailed off-line studies to interpolate between unstudied operating conditions, one can estimate the margins from the present operating point without employing detailed calculations. This project looked at general ways to improve the operator procedures with particular emphasis on estimating the margin based on such pattern matching schemes. As voltage security is an increasingly important issue as systems are operating under greater stress, this study focused on voltage issues.

Specific contributions from this study were:

- A typical set of operating procedures was tabulated into an on-line database. Conceptually, these margins can be easily modified on-line to reflect changing system conditions.
- Several pattern matching type approaches were investigated using a modified New England 39 bus system. Based on these results, a system based on feedforward artificial neural networks (ANN) was designed.
- A modified ANN system, employing multiple networks and a voting system, was applied to the Western System Coordinating Council (WSCC) system. The analysis was based on a WSCC 5000 bus model over a large range of loading conditions considering all major contingencies.
- Results on P margin estimations for the California Oregon Intertie showed no misclassifications of security and an average error of 1.2%.
- Results on P margin estimations for the California area showed no misclassifications of security and average error of 3.7%.

- A single estimator covering select multiple contingencies raised margin errors on the California Oregon Intertie to 5.8% but again there were no misclassifications of security. Conceptually, this situation represents a flexible multivariate nomogram.

The test results shown here establish that using a system of feedforward ANNs, one can accurately estimate security margins for on-line application. In practice, the operating schedules face the possibility of numerous combinations of operating conditions and equipment outages. To avoid a proliferation of estimators, it is important that a single network can perform well under some multiple contingencies. The results show that some such combinations can be solved using only one set of neural networks. Thus, one may be able to provide a complete system assessment with a manageably small number of networks, each trained for a limited set of multiple outages.

The overall effectiveness of the developed method depends largely on the credibility of the data. That is, to what extent does the data used for training represent the unstudied cases? For the voltage security assessment problem studied here, this condition appears to be satisfied. There is a trade-off between accuracy of the approach, number of networks and number of off-line studies. For practical implementation, this approach requires operation planners to increase somewhat the number of off-line studies, as well as systematically record data, so as to improve the estimates and where possible automate the analysis. Subsequent research efforts should investigate other security criteria that may be less amenable to interpolation. While estimating margins is useful, a broader objective is to use the system to not only calculate the margin but also to estimate transfer limits based on all security limits.

Table of Contents

1. Introduction

1.1 Background

A Modern Energy Management System (EMS) provides sophisticated online security analysis applications to assist operators in ensuring that the power system can survive credible contingencies. Still in current practice, system operators generally refer to written operating procedures to establish system constraints, particularly in regards to transfer limits across major interties. The limits are based on numerous power system studies that represent the stressed system and satisfy specific performance criteria following select contingencies. For example in the Western US, the determination of limits follows the guidelines of the Western System Coordinating Council (WSCC) as detailed in the "Procedures for Regional Planning Project Review and Rating Transmission Facilities" and WSCC's "Minimum Operating Reliability Criteria" [1]. These criteria include both dynamic and static performance measures. Under this approach, transfer ratings are typically conservative, as the off-line studies are based on highly stressed system conditions and incomplete, as these studies cannot analyze all combinations of equipment out-of-service.

In the Path 15 procedures (formerly referred to as S-5 procedures [2]), which were extensively studied here, outages and curtailment studies are performed to determine the maximum COI (California Oregon Intertie) and NOB (Nevada Oregon Border) limits. The procedures tabulate predetermined limits for specified contingencies on the 235kV and 500KV systems. For our studies, emphasis was placed on just two WSCC stability criteria relating to voltage security: real power and reactive power margin. Voltage security means the ability of a system, not only to operate stably, but also to remain stable following credible contingencies or load increases [3]. It often means the existence of considerable margin from an operating point to the voltage instability point following contingencies. The margin could be the real power transfer on a specific line, loading within an area, or reactive power margin at some buses in a studied area. Industry experience has shown that voltage stability analysis is often amenable to static analysis [3, 4]. Those static procedures were followed here.

1.2 Security margins

In general, VS margins are defined as the difference between the value of a Key System Parameter (KSP) at the current operating condition and at the voltage stability critical point. Different utilities use different KSPs that stem from two main categories:

a) PV-based KSPs, such as, an area load or power transfer across an interface, and
b) VQ-based KSPs, such as, reactive power injection at a bus or group of buses

The procedures and comparison of PV and VQ methodology are detailed in section 3.4. The voltage stability criterion defines a margin so that subsequent to contingencies the system can maintain voltage stability. In general, these margins need to be conservative to allow for approximations in analysis and to provide some leeway to operators as they respond to disturbances.

1.3 Literature review

The fundamentals of modeling power systems, specifically concentrating on voltage and reactive power topics, are covered well in [5, 6]. In [7], issues on power system static security analysis are introduced. This gives the background on the significant roles played by security analysis in modern bulk power system operation and control. The voltage stability problems have attracted numerous research efforts during the last decade and many voltage stability margins and indices have been proposed and used throughout the world for voltage security analysis (VSA). One category of voltage stability indices is based on eigenvalue and singular value analysis of the system Jacobian matrix [e.g., 8-10]. The idea is to detect the collapse point by monitoring the minimum eigenvalue or singular value of the system Jacobian, which becomes zero at the collapse point. With the analysis of the associated eigenvectors or singular vectors, one can determine the critical buses in the system by the right vector, and the most sensitive direction for changes of power injections by the left vector. However, the behavior of these indices is highly nonlinear; i.e., they are rather insensitive to system parameter variations. For large systems, this is also computationally expensive.

The more prominently applied methods in voltage stability analysis are those that try to define an index using the system load margin. The two most widely used are the real power margin, P, associated with the PV curve, and the reactive power margin, Q, associated with the VQ curve. The P margin can be calculated using the point of collapse method [11] or the power flow continuation method [12]. In [13], it is formulated as an optimization problem. For fast calculation of the P margin, Ejebe et al. [14] and Chiang et al. [15] proposed curve fitting methods to calculate the limit of the nose curve. Similarly, Greene et al. [16] proposed a sensitivity based linear/quadratic estimation method. While the Q margin is the most commonly used index in practice, there is limited literature on the fast calculation of Q margins. The traditional method to obtain the Q margin is the VQ curve stress test.

Alternatively, one can consider artificial intelligence methodologies applied to VSA to overcome the burden of computation. VSA using Artificial Neural Networks (ANNs) have been discussed in [17] demonstrating the ability to approximate a PV curve. In [18], the energy margin is used as an index for voltage stability assessment via ANNs and the energy margin sensitivities have been used to determine the candidate input variables for training an ANN. In [19], various parameters are studied as the candidates for input features. Critical branch flows and reactive reserve are indicated to be the key variables.

ANN design and determination of parameters is also of interest. A fast learning strategy that allows the optimal number of hidden neurons to be easily determined is proposed in [20]. Self-organizing networks have also been applied to VSA. In [21], a Kohonen neural network is used for on-line voltage collapse margin estimation. Margin to voltage collapse is in terms of the system loading distance of the operating point from the critical point. In [22], a Kohonen network is used as a front end of a combined network. The Kohonen network is used to extract the relevant features, and supervised learning identifies the features appropriate for voltage stability margin. In [23], self-organized ANNs are used for reduction of the system model and as an input set for multilayered ANN learning, while multilayered ANNs are used for detecting topology, and for monitoring and assessment of voltage stability. Section 3.3 details these developments further.

1.4 Organization of this study

This report first overviews neural network methodology, placing emphasis on network design. Of particular importance are the network parameters and selection of features. VSA is reviewed in section 3. The specific detailed steps in computing the P and Q margins are provided. These are used in the subsequent development. The New England 39 bus system is used to select the most promising approaches and to demonstrate the inability of simple regression methods to provide adequate estimates. Subsequently, the method is applied to the WSCC system. The results show the credibility of the method in estimating security margin and thus, to identify transfer limit on key interties.

2. Neural Network Overview

2.1 Introduction

2.1.1 Neural networks

The neural network was inspired from its inception by the recognition that the human brain computes differently than that of a conventional digital computer. The brain acts as a highly complex, nonlinear, and parallel computer. A neural network is a massively parallel distributed processor made up of simple processing units, known as neurons, which has a propensity for storing, and making easily available, experiential knowledge. It resembles the brain in two respects:

1. Knowledge is acquired by the network from its environment through learning processes.
2. Inter-neuron connection strengths, known as synaptic weights, are used to store the acquired knowledge.

The procedure used to set the connection strengths is called learning, the function of which is to modify the synaptic weights of the network in an orderly fashion to attain a desired design objective. A neural network derives its computing power through its massively parallel-distributed structure and its ability to learn and therefore generalize. Generalization refers to the neural network producing reasonable outputs for inputs not encountered during training (learning). These two information-processing capabilities make it possible for neural networks to solve complex problems. In practice, neural networks often cannot provide adequate solutions by working individually. Rather, they need to be integrated into a consistent system engineering approach. Specifically, a complex problem of interest is decomposed into a number of relatively simple tasks, and neural networks are assigned to a subset of the tasks that match their inherent capabilities. In this work, the neural networks method is integrated into a system approach for power system voltage security analysis.

2.1.2 Properties of neural networks

The use of neural networks offers the following useful properties and capabilities:

1. Nonlinearity. A neural network, made up of an interconnection of nonlinear neurons, is itself nonlinear. Moreover, the nonlinearity is of a special kind in the sense that it is distributed throughout the network. Most real systems, including power systems are nonlinear, so this property is very desirable for its applications in power systems.
2. Input-Output Mapping. A popular paradigm of learning called learning with a teacher or supervised learning involves modification of the synaptic weights of a neural network by applying a set of labeled training samples or task examples. Each example consists of a unique input signal and a corresponding desired response. The network learns from the examples by constructing an input-output mapping for the problem. In power system voltage security analysis, the traditional approaches which are widely used can be used to generate those training samples.
3. Adaptivity. Neural networks have a built-in capability to adapt their synaptic weights to changes in the surrounding environment. In particular, a neural network trained to operate in a specific environment can be easily retrained to deal with minor changes in the operating environmental conditions. Moreover, when it is operating in a nonstationary environment, a neural network can be designed to change its synaptic weights in real time.
4. Fault tolerance. A neural network has the potential to be inherently fault tolerant in the sense that its performance degrades gracefully under missing or erroneous data. The reason is that the information is distributed in the network, the errors must be extensive before catastrophic failure occurs.

These are the properties that are most desirable for solving the problems at hand. See [24] for a discussion of other useful properties.

2.1.3 The model of a neuron

A neuron is an information-processing unit that is fundamental to the operation of a neural network. Figure 2.1 shows a model of neuron. There are three basic elements:

1. A set of synapses or connecting links, each of which is characterized by a weight or strength of its own.

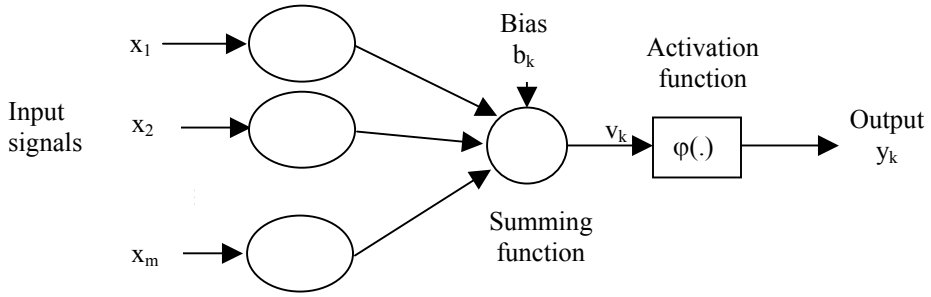

Figure 2.1: Model of a neuron

2. An adder for summing the input signals, weighted by the respective synapses of the neuron; the operations by the adder constitute a linear combiner.
3. An activation function for limiting the amplitude of the output of a neuron. Typically, it constrains the amplitude of the output signals to lie within the intervals [0, 1] or [-1,1].

The neuron in Figure 2.1 also includes an externally applied bias, denoted by b_k. The bias b_k has the effect of increasing, or lowering, the net input of the activation function, depending on whether it is positive, or negative. The activation function, denoted by $\varphi(v)$, defines the output of a neuron in terms of the induced local field v. There are basically three different kinds of activation functions:

1. Threshold function. $\varphi(v) = \begin{cases} 1 & \text{if} \quad v \geq 0 \\ 0 & \text{if} \quad v < 0 \end{cases}$
2. Piecewise-linear function. $\varphi(v) = \begin{cases} 1 & \text{if} \quad v \geq \frac{1}{2} \\ v & \frac{1}{2} > v > -\frac{1}{2} \\ 0 & \text{if} \quad v \leq -\frac{1}{2} \end{cases}$
3. Sigmoidal functions, including the logistic function: $\varphi(v) = \frac{1}{1+\exp(-av)}$, and the hyperbolic tangent function: $\varphi(v) = \tanh(v) = \frac{1-\exp(-v)}{1+\exp(v)}$, as shown in Figure 2.2 (a) and (b).

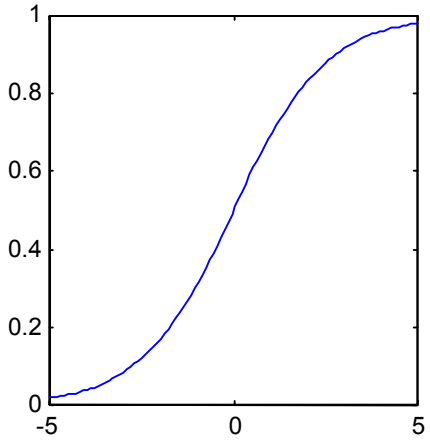

Figure 2.2 (a): Logistic function

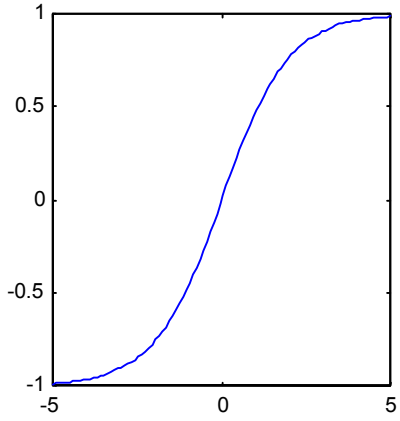

Figure 2.2 (b): Hyperbolic tangent function

2.2 Learning processes

Learning is a process by which the free parameters of a neural network are adapted through stimulation by the environment in which the network is embedded. The type of learning is determined by the manner in which the parameter changes take place. The property that is of primary significance for a neural network is the ability of the network to learn from its environment, and to improve its performance through learning. A neural network learns about its environment through an interactive process of adjustments applied to its synaptic weights and bias levels. Ideally, the network becomes more knowledgeable about the environment after each

iteration of the learning process. There are five basic learning rules: error-correction learning, memory-based learning, Hebbian learning, competitive learning, and Boltzmann learning.

2.2.1 Error-correction learning

Error-correction learning is based on optimum filtering and is used in feedforward networks, which are employed by this study. To illustrate the learning rule, consider the simple case of a neuron k constituting the only computational node in the output layer of a feed forward neural network, as depicted in Figure 2.3.

The output signal $y_k(n)$, representing the only output of the neural network, is compared to a desired response or target output, $d_k(n)$. Consequently, an error signal, $e_k(n)$, is produced, where $e_k(n) = d_k(n) - y_k(n)$. The error signal $e_k(n)$ actuates a control mechanism, the purpose of which is to apply a sequence of corrective adjustments to the synaptic weights of neuron k. The corrective adjustments are designed to make the output signal $y_k(n)$ approach the desired response $d_k(n)$ in a step-by-step manner. This objective is achieved by minimizing a cost function or index of performance, $\varepsilon(n) = 0.5\ e^2_k(n)$. That is, $\varepsilon(n)$ is the instantaneous value of the error energy. The step-by-step adjustments to the synaptic weights of neuron k are continued until the system reaches steady state (i.e., the synaptic weights are essentially stabilized). Minimization of the cost function $\varepsilon(n)$ leads to a learning rule commonly referred to as the delta rule or Widrow-Hoff rule:

$$\Delta w_{kj}(n) = \eta e_k(n)\, x_j(n) \tag{2.1}$$

where $w_{kj}(n)$ is the weight of neuron k excited by $x_j(n)$ of the signal vector $\boldsymbol{x}(n)$ at time step n. η is a positive constant that determines the rate of learning.

2.2.2 Memory-based learning

Memory-based learning operates by memorizing the training data explicitly. All (or most) of the past experiences are explicitly stored in a large memory of correctly classified input-output examples as $\{(\mathbf{x}_i, d_i)\}_{i=1}^{N}$, where $\mathbf{x}_i$ denotes an input vector and d_i denotes the corresponding desired response. All memory-based learning algorithms involve two essential ingredients:

(1) a criterion for defining the local neighborhood of the test vector $\mathbf{x}_{\text{test}}$, and,
(2) a learning rule applied to the training examples in the local neighborhood of $\mathbf{x}_{\text{test}}$.

In a simple, yet effective type of memory-based learning, known as the nearest neighbor rule, the local neighborhood is defined as the training example that lies in the immediate neighborhood of

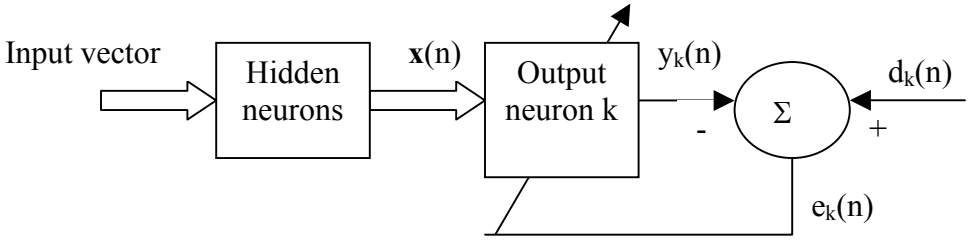

Figure 2.3: Feedback in network

the test vector $\mathbf{x}_{\text{test}}$. In particular, the vector $\mathbf{x}'_N \in \{\mathbf{x}_1, \mathbf{x}_2, ..., \mathbf{x}_N\}$ is said to be the nearest neighbor of $\mathbf{x}_{\text{test}}$ if $\min_i d(\mathbf{x}_i, \mathbf{x}_{test}) = d(\mathbf{x}'_N, \mathbf{x}_{test})$ where $d(\mathbf{x}_i, \mathbf{x}_{\text{test}})$ is the Euclidean distance between the vectors $\mathbf{x}_i$ and $\mathbf{x}_{\text{test}}$. The class associated with the minimum distance, that is, vector $\mathbf{x}_N'$, is reported as the classification of $\mathbf{x}_{\text{test}}$.

2.2.3 Hebbian learning

Hebb's postulate learning is the oldest and most famous of all learning rules; it is named in honor of the neuropsychologist Hebb. It has two parts [25]:

(1) If two neurons on either side of a synapse (connection) are activated simultaneously, then the strength of that synapse is increased.
(2) If two neurons on either side of a synapse are activated asynchronously, then that synapse is weakened or eliminated.

One form of Hebbian learning is using covariance hypothesis:

$$\Delta w_{kj} = \eta(x_i - \bar{x})(y_k - \bar{y}) \tag{2.2}$$

where η is the learning-rate parameter. $\bar{x}$ and $\bar{y}$ are the time-averaged values of the presynaptic signal, x_i, and postsynaptic, y_k, respectively. One can see from (2.2) that synaptic weight w_{ij} is enhanced if there are sufficient levels of presynaptic and postsynaptic activities. Synaptic weight w_{ij} is depressed if there is either a presynaptic activation in the absence of sufficient postsynaptic activation or a postsynaptic activation in the absence of sufficient presynaptic activation. There is strong physiological evidence for Hebbian learning in the area of the brain called the hippocampus. This physiological evidence provides Hebbian learning with significant justification.

2.2.4 Competitive learning

Competitive learning is also inspired by neurobiological considerations. The output neurons of a neural network compete among themselves to become active (fired). Whereas in a neural network based on Hebbian learning several output neurons may be active simultaneously, in competitive learning only a single output neuron is active at any one time. It is this feature that makes competitive learning highly suited to discover statistically salient features that may be used to classify a set of input patterns. The individual neurons of the network learn to specialize on ensembles of similar patterns; in doing so they become feature detectors for different classes of input patterns. The standard competitive learning rule defines change of weight by

$$\Delta w_{kj} = \begin{cases} \eta(x_j - w_{kj}) & \text{if neuron } k \text{ wins} \\ 0 & \text{else} \end{cases} \tag{2.3}$$

This rule has the overall effect of moving the synaptic weight vector w_k of winning neuron k toward the input pattern $\mathbf{x}$. This kind of learning is used in Kohonen maps which are briefly investigated in this work.

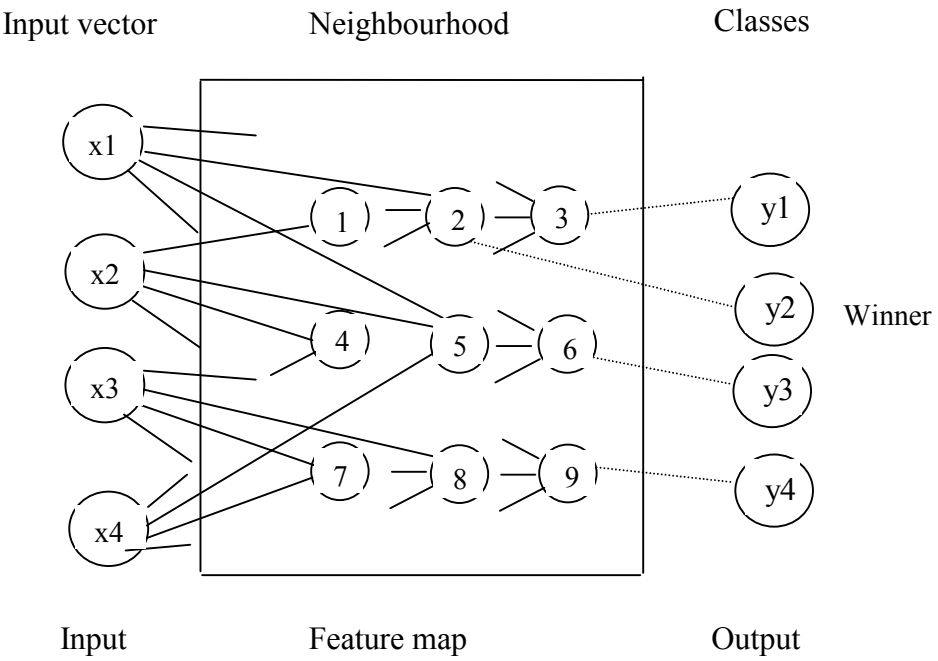

Figure 2.4: Kohonen networks

2.2.5 Bolzmann learning

The Boltzmann learning rule, named in honor of Ludwig Boltzmann, is a stochastic learning algorithm derived from ideas rooted in statistical mechanics. A neural network designed on the basis of the Boltzmann learning rule is called a Boltzmann machine. The machine is characterized by an energy function:

$$E = -\frac{1}{2}\sum_{j}\sum_{k} w_{kj} x_k x_j \qquad j \neq k \tag{2.4}$$

The machine operates by choosing a neuron at random at some step of the learning process, then flipping the state of neuron from state x_k to - x_k at some temperature T with probability $P = \frac{1}{1+\exp(-\Delta E_k / T)}$, where E_k is the energy change resulting from such a flip. If this rule is applied repeatedly, the machine will reach thermal equilibrium. The learning rule is defined by

$$\Delta w_{kj} = \eta(\rho_{kj}^{+} - \rho_{kj}^{-}), \quad j \neq k \tag{2.5}$$

where ρ_{kj}^{+} and ρ_{kj}^{-} denote the correlation between the states of neurons k and j with the network in its clamped condition (visible neurons are all fixed into specific states determined by the environment) and free-running condition, respectively.

2.3 Kohonen self-organizing networks

Kohonen self-organizing networks [26, 27] are competitive-based network paradigm for data clustering. Networks of this type impose a neighborhood constraint on the output units, such that a certain topological property in the input data is reflected in the output units' weights. Figure 2.4 shows a Kohonen network. Based on competitive learning, Kohonen networks use a similarity measure. The winning unit is considered to be the one with the largest activation. For Kohonen feature maps, however, one updates not only the winning unit's weights but also all of the weights in a neighborhood around the winning units. The neighborhood's size generally decreases slowly with each iteration. A sequential description of how to train a Kohonen self-organizing network is as follows:

(1) Select the winning output unit as the one with the largest similarity measure between all weight vectors $\mathbf{w}_i$ and the input vector $\mathbf{x}$. If the Euclidean distance is chosen as the dissimilarity measure, then the winning unit c satisfies the following equation:

$$\|x - \mathbf{w}_c\| = \min_i \|x - \mathbf{w}_i\| \tag{2.6}$$

(2) Let NB_c denote a set of indices corresponding to a neighborhood around winner c. The weights of the winner and its neighboring units are then updated by:

$$\Delta w_i = \eta(\mathbf{x} - \mathbf{w}_i) \quad i \in NB_c \tag{2.7}$$

Instead of defining the neighborhood of a winning unit, one can also use a neighborhood function $\Omega_c(i)$ around a winning unit c. For instance, the Gaussian function can be used as the neighborhood function:

$$\Omega_c(i) = \exp\left(\frac{-\|p_i - p_c\|^2}{2\sigma^2}\right) \tag{2.8}$$

where p_i and p_c are the positions of the output units i and c, respectively, and σ reflects the scope of the neighborhood. By using the neighborhood function, the update formula can be rewritten as:

$$\Delta w_i = \eta\Omega_c(i)(\mathbf{x} - \mathbf{w}_i) \tag{2.9}$$

where i is the index for all output units.

To achieve better convergence, the learning rate and the size of neighborhood should be decreased gradually with each iteration.

2.4 Multilayer perceptron

2.4.1 Introduction

Multilayer perceptron network consists of a set of sensory units (source nodes) that constitute the input layer, one or more hidden layers of computation nodes, and an output layer of computation nodes. The input signal propagates through the network in a forward direction, on a layer-by-layer basis. Figure 2.5 shows a multilayer perceptron. Multilayer perceptrons have been applied successfully to solve a number of diverse and difficult problems by training them in a supervised manner with a highly popular algorithm known as the back-propagation algorithm. This algorithm is based on the error-correction learning rule. Error back-propagation learning consists of two passes through the different layers of the network: a forward pass and a backward pass. In the forward pass, an activity pattern (input vector) is applied to the sensory nodes of the network, and its effect propagates through the network layer by layer. Next, a set of outputs is produced as the actual response of the network. During the forward pass the synaptic weights of the networks are all fixed. During the backward pass, on the other hand, the synaptic weights are all adjusted in accordance with an error-correction rule. Specifically, the actual response of the network is subtracted from a desired response to produce an error signal. This error signal is then propagated backward through the network against the direction of synaptic connections-hence the name "error back-propagation." The synaptic weights are adjusted to make the actual response of the network move closer to the desired response in a statistical sense.

2.4.2 Error back-propagation algorithm

The backpropagation algorithm is defined using delta rule:

$$\Delta w_{ji}(n) = \eta \delta_j(n) y_i(n) \tag{2.10}$$

where $y_i(n)$ is the input signal of neuron j from neuron i and $\delta_j(n)$ is the local gradient. If neuron j is an output node, $\delta_i(n)$ equals the product of the derivative $\varphi_j'(v_j(n))$ and the error signal $e_j(n)$, both of which are associated with neuron j, i.e., $\delta_j(n) = e_j(n)\varphi_j'(v_j(n))$. If neuron j is a hidden node, $\delta_i(n) = \varphi_j'(v_j(n))\sum_k \delta_k(n) w_{kj}(n)$, i.e., $\delta_i(n)$ equals the product of the associative derivative $\varphi_j'(v_j(n))$ and the weighted sum of the δ's computed for the neurons in the next hidden or output layer that are connected to neuron j. The factor $\varphi_j'(v_j(n))$ depends solely on the activation function associated with hidden neuron j. Figure 2.6 shows the signal-flow graph of the error

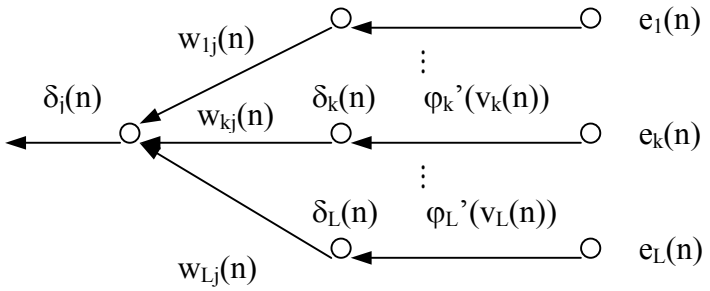

Figure 2.6 Signal-flow graph of the error back-propagation algorithm

back-propagation algorithm.

2.4.3 Achieving better performance

There are many methods that will significantly improve the back-propagation algorithm performance. A few are briefly described here:

(1) The sequential mode of back-propagation learning is computationally faster than the batch mode. This is especially true when the training data set is large and highly redundant.
(2) The use of an example that results in the largest training error or an example that is radically different from all those previously used. This will maximize information content. These two heuristics are motivated by a desire to search more of the weight space.
(3) Generally, using an antisymmetric activation function is faster than using nonsymmetric functions in back-propagation.
(4) Normalizing the inputs and target values will keep the back-propagation algorithm away from the limiting value of the sigmoid activation function. Otherwise, the back-propagation algorithm tends to drive the free parameters of the network to infinity, and thereby slow down the learning process by forcing the hidden neurons into saturation. The input should be uncorrelated; this can be done using principal component analysis. The decorrelated input should be scaled so that their covariances are approximately equal, thereby ensuring that the different synaptic weights in the network learn at approximately the same speed.
(5) A good choice of initialization is important so that too large a value will not drive the network to saturation nor too small a value will cause the network to operate on a very flat area around the origin of the error surface.
(6) A high learning rate will speed up the rate of learning, but the network may become unstable. A simple way of increasing the rate of learning yet avoiding the danger of instability is to modify the delta rule by including a momentum term:

$$\Delta w_{ji}(n) = \alpha \Delta w_{ji}(n-1) + \eta \delta_j(n) y_i(n) \tag{2.11}$$

where α is usually a positive number called the momentum constant.

2.4.4 Improving generalization

The essence of back-propagation learning is to encode an input-output mapping into the synaptic weights and thresholds of a multilayer perceptron. The hope is that the network becomes well trained so that it learns enough about the past to generalize to the future. One problem that occurs during training is called overfitting. The error on the training set is driven to a very small value, but when new data is presented to the network the error is large. The network has memorized the training examples, but it has not learned to generalize to new situations. Use a network that is just large enough to provide an adequate fit will improve network generalization. The larger a network is used the more complex the functions that the network can create. If a small enough network is used, it will not have enough power to overfit the data. The problem is that it is difficult to know beforehand how large a network should be for a specific application.

There are two other methods for improving generalization. The first is modifying the performance function, which is normally chosen to be the sum of squares of the network errors on the training set:

$$F = mse = \frac{1}{N}\sum_{i=1}^{N}(e_i)^2 \tag{2.12}$$

The modified performance function is then:

$$msereg = \gamma mse + (1-\gamma)msw \tag{2.13}$$

where γ is the performance ratio, and $msw = \frac{1}{n}\sum_{j=1}^{n} w_j^2$.

Using such a performance function will cause the network to have smaller weights and biases, and this will force the network response to be smoother and less likely to overfit. Another method for improving generalization is early stopping. In this technique, the available data is divided into three subsets: training set, validation set and test set. The training set is used for computing the gradient and updating the network weights and biases. The error on the validation set is monitored during the training process to guard against overfit. The validation error will normally decrease during the initial phase of training, as does the training set error. When the network begins to overfit the data, the error on the validation set will typically begin to rise and learning can be stopped. Both methods are used in this work to guard against overfitting.

2.4.5 Principal component analysis

In some situations, the dimension of the input vector is large, but the components of the vectors are highly correlated (redundant). It is useful in this situation to reduce the dimension of the input vectors. An effective procedure for performing this operation is principal component analysis. This technique has three effects: it orthogonalizes the components of the input vectors so that they are uncorrelated with each other; it orders the resulting orthogonal components so that those with the largest variation come first; and it eliminates those components which contribute the least to the variation in the data set. In the study, this technique is used along with engineering knowledge to assist in the feature selection.

3. Voltage Security Analysis (VSA)

3.1 Introduction

3.1.1 Voltage collapse

Voltage collapse is a system instability that involves several power system components simultaneously. It typically occurs on power systems that are heavily loaded, faulted and/or have reactive power shortages. This occurs since voltage collapse is associated with the reactive

power demands of loads not being met due to limitations on the production and transmission of reactive power. The production limitations include generator and SVC reactive power limits and the reduced reactive power produced by capacitors at low voltages. The primary limitations in transmission are high reactive power losses on heavily loaded lines and line outages. Reactive power demands may also increase due to changes in the load such as, motor stalling or increased proportion of compressor load.

Voltage collapse takes place on the different timescales ranging from seconds to hours, specifically:

(1) Electromechanical transient (e.g., generators, regulators, induction machines) and power electronic (e.g. SVC, HVDC) phenomena in the time range of seconds.
(2) Discrete switching devices, such as, load tapchangers and excitation limiters acting at intervals of tens of seconds.
(3) Load recovery processes spanning several minutes.

In this study, we analyze (2) and (3) which are so called "long term" time scale events. There are numerous power system events known to contribute to voltage collapse.

- Increase in loading
- Generators or SVC reactive power limits
- Action of tap changing transformers
- Load recovery dynamics
- Line tripping or generator outages

Most of these changes have a large effect on reactive power production or transmission. Control actions such as switching in shunt capacitors, blocking tap changing transformers, redispatch of generation, rescheduling of generator and pilot bus voltages, secondary voltage regulation, load shedding and temporary reactive power overload of generators are countermeasures against voltage collapse. Machine angles are typically also involved in the voltage collapse. Thus, there is no sharp distinction between voltage collapse and classical transient instability. The differences between voltage collapse and classical transient instability are those of emphasis: voltage collapse focuses on loads and voltage magnitudes whereas transient instability focuses on generators and angles. Also, voltage collapse often includes longer time scale dynamics and includes the effects of continuous changes such as load increases in addition to discrete events such as line outages.

Increasing voltage levels by supplying more reactive power generally improves the margin to voltage collapse. In particular, shunt capacitors become more effective at supplying reactive power at higher voltages. Increasing voltage levels by tap changing transformer action can decrease the margin to voltage collapse by in effect increasing the reactive power demand. Still, voltage levels are a poor indicator of the margin to voltage collapse. While there are some relations between the problems of maintaining voltage levels and voltage collapse, they are best regarded as distinct problems since their analysis is different and there is only partial overlap in the control actions used to solve both problems.

3.1.2 Voltage collapse indices

There are numerous indices to indicate proximity to voltage collapse that have been studied. The following is a brief introduction to these indices:

(1) Sensitivity factors
Sensitivity factors are indices used in several utilities throughout the world to detect voltage stability problems and to decide corrective measures [28, 29]. These indices were first used to predict voltage control problems in generator QV curves, and may be defined as

$$VSF_i = \max_i \left\{ \frac{dV_i}{dQ_i} \right\} \tag{3.1}$$

where VSF stands for Voltage Sensitivity Factor. As generator *i* approaches the bottom of its QV curve, the value of VSF_i becomes large and eventually changes sign, indicating an unstable voltage control condition.

(2) Singular values
Singular values of a reduced matrix can be used to determine proximity to voltage collapse. Let

$$\Delta Q = J_{QV} \Delta V \tag{3.2}$$

with

$$\det J_{QV} = \frac{\det J}{\det J_1} \tag{3.3}$$

where J is the Jacobian in power flow equations and J_1 is the real power sensitivities to angle deviations, i.e., $\left[\frac{\partial P}{\partial \delta} \right]$. The singular values of this reduced matrix can be used to determine proximity to voltage collapse.

(3) Second order performance indices
Indices based on first order information (linearizations), such as singular values and eigenvalues and several other indices presented in this document, may be inadequate to predict proximity to collapse as they neglect large discontinuities in the presence of system control limits like generator capability or transformer tap limits, as previously discussed. Conversely, it is possible to calculate a second order index that exploits additional information embedded in these indices to overcome some of these discontinuities [30].

(4) Energy function
Energy function, a technique based on Lyapunov stability theory, is used for both transient stability and voltage stability analysis. In this approach, power system stability is like a ball, which lies at the bottom of a valley. The stability can be understood as the ball settling to the bottom of a uneven surface when there is a disturbance. As the power system changes, the landscape of this surface and the ridges surrounding the indentations change. A voltage collapse corresponds to a ridge being sufficiently lowered so that with a small perturbation the ball can

roll from the bottom of one indentation to a neighboring area. The height of the lowest ridge can be computed and used as an index to monitor the proximity to voltage collapse [31].

(5) Loading margin

For a particular operating point, the amount of additional load in a specific pattern of load increase that would cause a voltage collapse is called the loading margin to voltage collapse. Loading margin is the most basic and widely accepted index of voltage collapse. If system load is chosen to be the parameter, which varies, then a system PV curve can be drawn. In this case, the loading margin to voltage collapse is the change in loading between the operating point and the nose of the curve. The advantages of the loading margin as a voltage collapse index are [32]:

- The loading margin is straightforward, well accepted and easily understood.
- The loading margin is not based on a particular system model; it only requires a static power system model and can be supplemented with dynamic system models.
- The loading margin is an accurate index that takes full account of the power system nonlinearity and limits such as reactive power control limits encountered as the loading is increased. Limits are not directly reflected as sudden changes on the loading margin.
- Once the loading margin is computed, it is easy and quick to compute its sensitivity with respect to any power system parameters or controls.

The computational costs are the most serious disadvantage of the loading margin and make it unsuitable for on-line use. This work applies neural networks to overcome this drawback to estimate margin in order to be used on-line. There are numerous other indices for voltage security. The reader is referred to [31] for more details.

3.1.3 Assessing voltage stability

Voltage stability is a serious concern, which must be examined during planning and operational studies. Voltage stability margin is a measure of how close the system is to voltage instability. The approach need to assess margin will differ slightly between off-line studies (such as operation planning) and on-line studies (such as application of on-line voltage stability assessment tools in the EMS environment). In the off-line environment, such as operation planning, it is necessary to determine the margin for all design contingencies (such as single element outages, double outages of lines on the same corridor) for system conditions with all elements in service and for conditions with one or more elements out-of-service. Studying conditions with one component out-of-service is necessary to provide margin for the uncertainty of operating conditions. Often, for study purposes, each out-of-service element is combined with each design contingency, to form a set of double contingencies [2].

For on-line studies, the system state and topology is known (or at least approximately known) through system measurements and state estimation. Therefore, it is necessary to study only the criteria contingencies for all elements in service. As a result, fewer scenarios need to be examined and less margin may be required than for off-line studies in which the system uncertainty is greater. One important aspect of practical VS assessment is the consistency between on-line and off-line assessment methods.

In theory, either power flow based (static) tools, such as the Voltage STABility program (VSTAB) [33], or time-domain simulation (dynamic) tools, such as the Extended Transient/Midterm Stability Program (ETMSP) [34], or the so-called Quasi-Dynamic (or Fast

Time-Domain) simulation programs [35], can be used to calculate system VS margins. The dynamic tools must have appropriate models for the study of voltage stability, such as overexcitation limiters, thermostatically controlled loads and timing of ULTC tap movements.

The VS margins calculated using different tools should be very close, provided that consistent device models are used in the two programs and that voltage instability does not occur during the transient period. Unfortunately, because of the high CPU time requirements for time-domain simulation, it is impractical to calculate VS margins for all the contingency cases in this manner. A practical approach is to use a power flow based tool to calculate VS margins for the base case and all contingency cases, and use time-domain simulation only to bench mark the power flow results, and to determine the chronology of voltage instability, following a few selected critical contingencies.

3.2 Traditional VSA methods

Historically, power system engineers have used two main classes of programs for analysis of bulk power system performance: power flow and transient stability. Typically, voltage, active power and reactive power flow problems have been analyzed using static power flow programs. This approach was satisfactory since these problems have been governed by essentially static or time-independent factors. Power flow analysis allows simulation of a snapshot in time, such as, after automatic device actions but before operator intervention. Static analysis involves only the solution of algebraic equations and therefore is computationally much more efficient than dynamic analysis. Static analysis is preferred for the bulk of studies in which voltage stability limits for many pre-contingency and post-contingency cases must be determined.

Dynamic issues, such as first swing transient stability problems, have normally been addressed using a transient stability program. These programs ordinarily include dynamic models of the synchronous machines with models of the excitation systems, power system stabilizers (PSS), turbines and governors, as well as other dynamic models, such as loads, High Voltage Direct (HVDC) Current transmission, Static Var Compensators (SVC) and other fast acting devices. These component models and the accompanying solution algorithm are suitable for analysis of phenomena from tens of milliseconds (e.g., machine subtransient dynamics) up to several seconds or tens of seconds. Dynamic analysis provides the most accurate replication of the time responses of the power system. Accurate determination of the time sequence of the different events leading to system voltage instability is essential for post-mortem analysis and the coordination of protection and control. However, time-domain simulations are time consuming both in terms of CPU time and engineering effort required for analysis of results. Also, dynamic analysis does not readily provide information regarding the sensitivity or degree of instability. These may make dynamic analysis impractical for examination of a wide range of system conditions or for determining stability limits unless combined with other techniques. New computer programs and algorithms are constantly under development in order to relieve such limitations. For example, there are commercially available software packages that combine advance time-domain simulation techniques (e.g., those with variable step size) and other (e.g., eigenvalue analysis) techniques.

There is also the recent emergence of a new class of computer simulation software that provides utility engineers with powerful new tools for analysis of long-term dynamic phenomena. The ability to perform long-term dynamic simulations either with detailed dynamic modeling or

simplified quasi-steady-state modeling permits more accurate assessment of critical power system problems over longer time frames than is possible with conventional techniques.

3.3 Artificial intelligence methods in VSA

Numerous applications of artificial intelligence methods to power system security have been reported. A review of some recent examples with an emphasis on VSA is detailed in the following. For contingency studies, a combined fuzzy logic and probability based approach is suggested for ranking of contingencies for power system real time steady-state security evaluation [36]. An expert system has been developed to apply operational planning knowledge to the static security assessment problem. The expert system performs the contingency selection and remedial action tasks usually conducted off-line by an operational planner. Rule based techniques are used to select contingencies expected to cause steady state bus voltage violations [37].

In VSA, a neuro-fuzzy network is proposed for voltage security monitoring (VSM) using synchronized phasor measurements as input patterns [38]. A decision tree methodology is proposed in [39] to tackle voltage security concerns under two distinct situations, namely preventive and emergency. An expert system for enhancing both the voltage security and the voltage stability in power systems is presented in [40]. The expert system is implemented to improve the voltage profile when contingencies are less severe and to adopt appropriate control actions to prevent the system from collapsing when severe contingencies are encountered. A proposed fuzzy linear programming method employed various membership functions pertaining to constraints and cost functions of system models for voltage/reactive power control in [41].

For volt/var control in distribution systems, an adaptive neuro-fuzzy inference system (ANFIS) was presented [42]. The control objectives are minimization of system losses without violating the voltage security of the system. Power loss and voltage sensitivities obtained for the base case load flow are used to determine the dominant inputs to the fuzzy expert system. The rules are adapted using a neural network. A new approach using fuzzy set theory for voltage and reactive power control of power systems is presented in [43]. The purpose is to enhance voltage security of an electric power system. The violation bus voltage and the controlling variables are translated into fuzzy set notations to formulate the relation between voltage violation level and controlling ability of controlling devices. A knowledge-based fuzzy approach is proposed to evaluate the dynamic voltage security including both voltage collapse and unacceptable voltage profiles following disturbances. The dynamic voltage-stability behavior of the power system, however complex and nonlinear in nature, is mapped into a fuzzy severity index by means of approximate fuzzy reasoning and a series of fuzzy calculus [44]. An architecture based on a suite of AI technologies and three-dimensional PQV surfaces, which provides prediction of local voltage collapse and indices of system voltage security, is presented in [45].

For improving voltage security, [46] uses fuzzy logic to model the operator's decision-making process while using sensitivity analysis to derive the necessary movements in control settings within an expert system that seeks a low cost, low number-of-controllers solution. In [47], the optimal reactive power compensation problem is considered as combinatorial optimization problem and a genetic algorithm (GA) is used for its solution. By combining three classes of learning methods, namely machine learning, artificial neural networks and statistical patter recognition, in a tool box, the large statistical data bases of voltage security information was

exploit optimally [48]. In [49], a neural network-based tool is proposed to provide on-line preventive control strategies capable to restore a multi-area power system to a secure operating point when a voltage instability condition is going to be reached. These strategies are, respectively, based on reactive power control actions, generating nodes voltage-magnitude control actions and load curtailment actions. In [50], simulated annealing (SA) is applied to search for the final global optimal solution for appropriate reactive power planning in order to enhance security of an electric power systems. The control strategy is expressed by simple rules, which measure the proximity of system state to certain operating conditions, and utilize linear equations to obtain the effective control models [51]. In order to minimize the fuel costs and to maximize the security measure of power systems in terms of limits on active and reactive power outputs of compensating devices, transformer tap setting, and bus voltage levels, a genetic algorithm (GA) based approach was proposed to solve the combined active and reactive power dispatch problem [52].

3.4 PV-based and VQ-based margin computation

The PV-based and VQ-based margins are the two most widely used static methods for VS assessment [6]. The methodology that should be followed for development of a full P-V curve for studies involving load areas is described below [4].

1. Choose a region as the study area wherein load will be incrementally increased. This could be a region that is suspected or known to be susceptible to voltage collapse. The quantities that will be varied are internal load and external generation.
2. Model the loads in the study area initially at a level of approximately 20% of the expected peak load. Generation external to the study area should be reduced to match the scaled down load levels in the study area. As loads are scaled up in the study area, the effects of increased load requirements on the study region's voltage profile will be captured.
3. Set the internal study area generation to a constant level of the on-line units. The real power output of the internal generators should remain unchanged during the P-V analysis. The reactive power capability of each of the generating units should represent the unit's capability, and the reactive power output of each unit should be allowed to adjust as the P-V analysis progresses. Voltage collapse will occur in the study region after the VAR capability in the study region is depleted.
4. Choose the bus or buses in the study area at which the voltages will be monitored as the power transfers into the study area are increased. As an initial investigation of a region for voltage instability, the engineer should select several buses to monitor. The monitored voltages are the y-axis data of a P-V curve. See VQ method step 2 regarding methods of identifying buses to monitor.
5. Determine (a) if the x-axis data will be load or interface flows, and (b) if the units will be MW or MVA. If an interface path is used, it should be defined in a manner that measures all imports to the receiving region.
6. Choose the system condition to be simulated. The system condition should be represented before internal loads and external generation are scaled up to develop the P-V data. A pre-contingency P-V analysis of the system provides an indication of the maximum capability of the study region to serve load. Simulating contingencies based on the stability criteria are required to assure compliance with the voltage stability margins and

provide information regarding the steady-state operating point that will occur after the contingency.

7. Solve the initial power flow case representing a low receiving area using the post-transient methodology.
8. Record the bus voltages at the monitored buses, and the load level or interface transfer level at which the power flow case was solved.
9. Scale loads and external generation up to match the load increase. The load increases can be larger at lower load levels than at higher load levels, which are near the point of collapse. Ensure that loads are scaled up in the neighboring systems if they have similar climatic or geographic characteristics to the system under study.
10. The results of the P-V analysis may indicate that the voltage profile of a region is significantly lower than acceptable operating conditions at the point-of-collapse. In such cases, the limit of the system could be determined by other voltage criteria, such as post-transient voltage deviation or the lower limit of acceptable operating voltage. However, in some receiving regions, typically regions with a high degree of shunt compensation, the point-of-collapse will occur at or near bus voltages that appear acceptable. For these cases, the system should be designed with some operating margin from the point of collapse.

The standard procedure for conducting voltage collapse analysis based on V-Q curves is as follows [4]:

1. Establish a power flow case representing the system's post-disturbance condition.
2. Identify the critical bus (also referred to as the weakest bus) in the system for this contingency. This is usually the most reactive deficient bus and typically, depends on the contingency. The weakest bus is the one that exhibits one of the following conditions under the worst single or multiple contingency: (a) has the highest voltage collapse point on the V-Q curve, (b) has the lowest reactive power margin, or (c) has the highest percentage change in voltage. It can be found using V-Q curve or the dV/dQ from the Jacobian (the bus that has the largest value for dV/dQ before collapse is the weakest bus). In this study, both methods are used.
3. Apply a fictitious synchronous condenser at the weakest bus.
4. Vary the condenser scheduled output voltage in small steps (say, 0.01pu).
5. Re-solve the power flow.
6. Record the bus voltage (V) and the reactive output of the condenser (Q).
7. Repeat steps 4 to 6 until sufficient points have been collected.
8. Use the V-Q curve to determine if there is sufficient margin.

The minimum point of this curve (where $dQ/dV = 0$) is the critical point; i.e., all points of the curve to the left of the minimum are assumed to be unstable, and those to the right to be stable.

Since voltage instability is due to a shortage of reactive supply to a bus or coherent bus group, the structural stress test used must assess when and why a shortage of reactive supply exists. A V-Q curve, being a reactive power voltage relationship, stresses the system in a manner similar to how the voltage instability occurs. Thus, a V-Q curve is better suited for this purpose since it directly assesses shortage of reactive supply. A P-V curve, however, is quite useful in assessing transfer or loading limits, thus is also used as a supplement. Using both methods is a requirement of WSCC.

3.5 Proposed pattern matching approaches to VSA

In this section, three different pattern matching approaches for estimating the MVAr margin are compared: linear regression, a Kohonen network and a feedforward ANN. For the following study, the New England 39 bus system has been modified to represent a system with different zones and critical interfaces. The system is divided into two zones, one load center with only load buses, and the other includes both load and generation buses. Figure 3.1 shows that the load center includes buses 17,18 and 27. The three tie lines are 3-18, 16-17 and 26-27. The focus of our study here is the buses within this load center. The training and testing data comes from the traditional V-Q method result. There are six data sets for training and testing: base case data and then five different loadings that represent increased load over the base case. For each data set there are 49 cases which represent one base case and all 48 n-1 contingencies. The total load for the base case is 6000 MW. The five different loadings are given by increasing load in steps of 400 MW with the most constrained case loaded at 8000 MW. For all these cases, weakest bus and reactive power margin are computed and the operating data for the selected features are recorded.

3.5.1 Regression method

Perhaps the most straightforward pattern matching method is to use a simple regression model. Standard statistical methods are used to select features from the study data and to best fit a curve to that data. Table 3.1 lists the correlation coefficients between line flows and MVAr margin. The first column shows the line flows of interest. This includes tie lines, lines connecting weakest buses, some lines near the load center and total tie line flow. The second column is the correlation coefficients between listed line flows and MVAr margin.

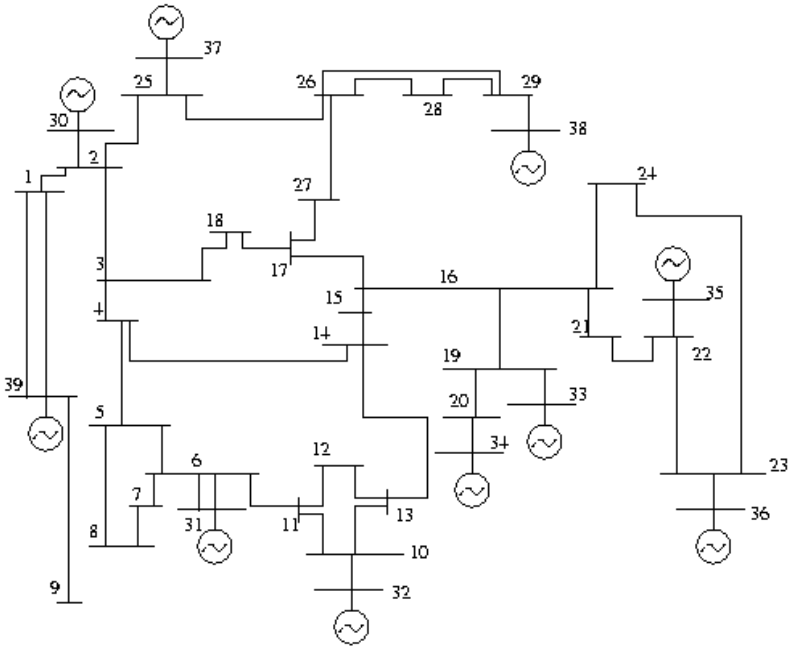

Figure 3.1 New England 39 bus system

Line	Original	Modified
tie lines*	-0.6386	-0.4468
03-18*	-0.4356	-0.4331
16-17*	-0.1031	-0.2035
17-18*	0.0766	-0.0889
17-27*	-0.0781	-0.1915
26-27*	-0.2250	-0.3444
25-26	0.0271	0.0689
02-03	-0.0554	-0.0029
14-15	0.0472	0.0523
15-16	-0.0123	-0.0266
16-19	-0.0195	0.0151
16-21	-0.1020	-0.0459

* selected feature set

Table 3.1 Correlation coefficients between line flows and MVAr margin

As can be seen from the table, the correlation coefficient between lines 17-18 or 17-27 and the margin are very small. Yet, we find that outage of 17-18 or 17-27 are among the worst of the contingencies (in the sense of MVAr margin loss). Such outages must be accounted for in the feature set. Most simply one could add a feature indicating various outages. For the purposes of training simplicity, we instead modified the line flow data by replacing all line outage flows (i.e., 0) with a large number (say, 500 MW). The correlation coefficients after this modification are listed in the third column of Table 1. The first six rows have the highest correlation coefficients and are our selected feature set (critical paths). A second order regression model is then used. Specifically, let the reactive margin, Q_m, be modeled by the polynomial

$$Q_m = P^T AP + B^T P + c \tag{3.4}$$

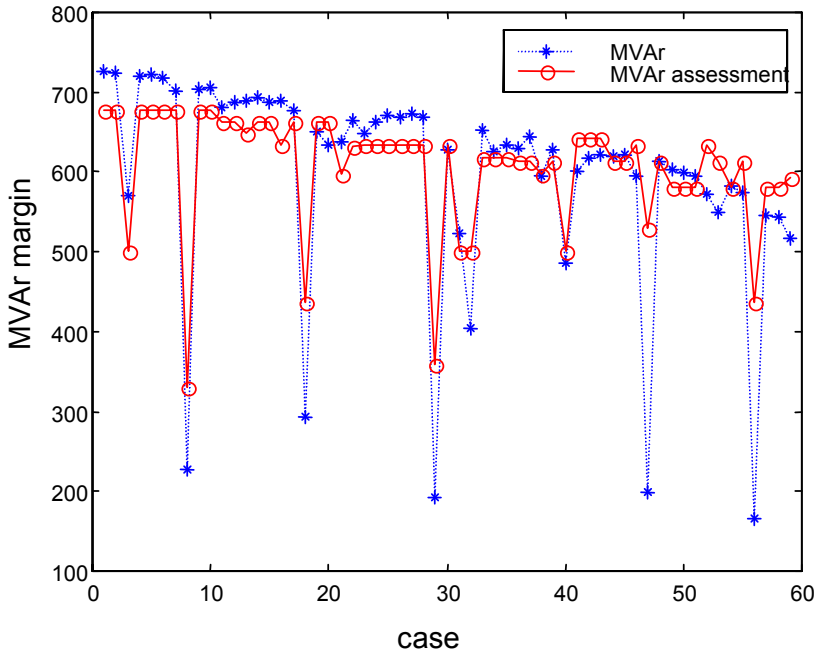

Figure 3.2 MVAr margin assessment using regression method

where A, B and c are model parameters, and $P = \{P_{ij}\}$, with P_{ij}, the power flow on critical paths.

The training and testing data comes from the power flow of the different cases. For each test, margins for all contingencies are precisely computed and compared to the estimate. The average error in margin estimate is 90.34 MVAr with a maximum error of 192.59 MVAr among the 20 tests. The standard deviation is 83.71 MVAr. Figure 3.2 shows one such test result. For large margins, the result is reasonable, but for small margins, the assessment is not satisfying. In the worst case, the error is more than 500 MVAr.

3.5.2 Kohonen network method

The Kohonen network looks for clusters in the data in order to develop an ordered mapping that reveals existing similarities in the inputs. In this work, two Kohonen maps were used to assess the reactive power margin of the 39 bus system. The two maps have the same size (10x10). The nodes in the first map have six fields, which are the real power flows of the critical lines. The nodes in the second map are the reactive power margins. In this way, the first map acts as the clustering mapping, and the second map act as an associative memory, which contains the margin information.

Again, the system is analyzed using 20 random tests. The average error is 103.71 MVAr and the maximum error is 145.85 MVAr. The standard deviation is 101.06 MVAr. The results are slightly worse than that of the regression method. The training speed is also much slower than that of the regression method. As we know, Kohonen map is mainly for unsupervised learning, where other methods such as regression method cannot be implemented. Results are illustrated in Figure 3.3.

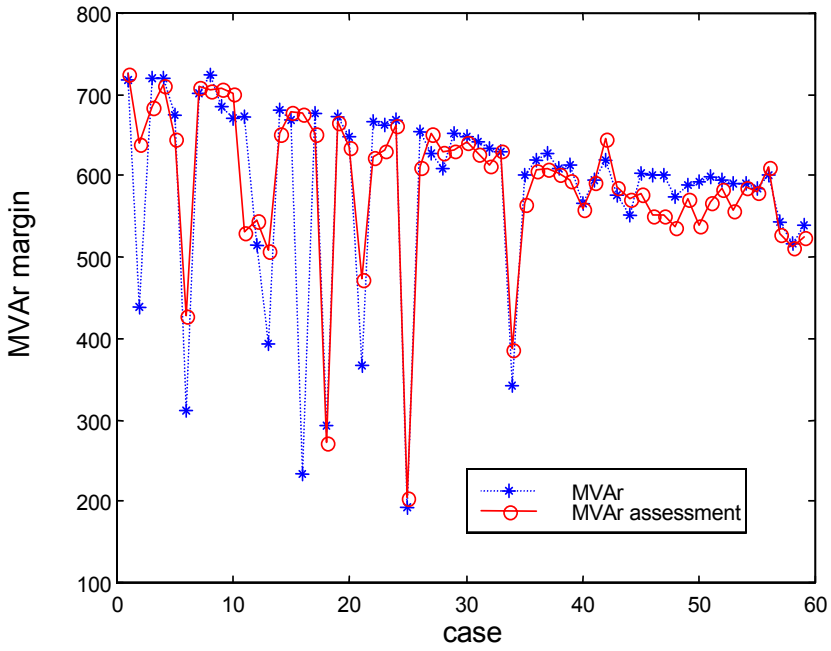

Figure 3.3 MVAr margin assessment using Kohonen maps

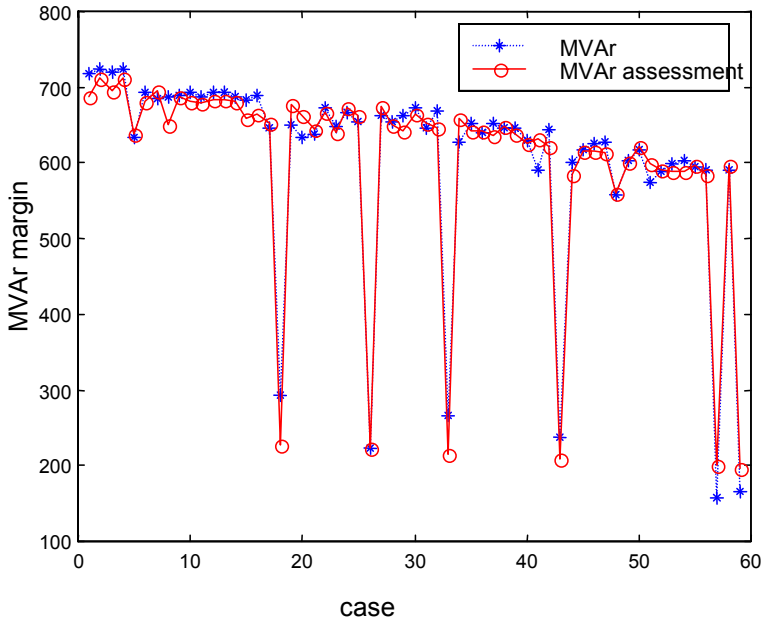

Figure 3.4 MVAr assessment using feedforward network(modified data)

3.5.3 Feedforward ANN method

In this section, a feedforward ANN with backpropagation method employing the Levenberg-Marquardt algorithm is investigated. General discussion of the backpropagation network is referred to the literature [24] and to the earlier discussion in section 2 and for the Levenberg-Marquardt algorithm to [53]. Two different sets of features are studied and results are compared. These two different sets are 6 original line flows and modified ones (see Figure 3.1). The selection is based on the contingency study and correlation coefficients. The worst n-1 contingency (in the reactive power margin sense) is the best candidate for the line flow feature. (e.g., if line 17-27 outage is the worst contingency, the flow of that line is chosen as the feature). Modification of line flows (see 3.1) is made in the second feature set.

The data set is divided into a training, validating and testing set. The training takes 80% of the data, 20% of which are for validation. The remaining 20% are for testing. Since the smaller the margin, then the worse the contingency, accurate estimation on small margins is most important. Using the modified data as discussed in 3.5.1, the result shown in Figure 3.4 is obtained. The largest error in the test case is 70MVAr. The average error is 23.89 MVAr and the maximum error is 35.03 MVAr. The standard deviation is 22.76 MVAr Besides the reactive margin, the ANN was also used to predict the weakest bus within the load center. The correct prediction rate in preliminary tests lay between 87% and 98%. Such information is useful for scheduling applications and will be the basis for further investigations.

3.6 Remarks

The test results show that using feedforward ANN network in reactive power margin assessment is promising. For the problem at hand, it appears that without introducing additional complications neither the Linear regression method nor the Kohonen map is capable of accurate estimates for the low margin cases.

4. Estimating Margins on the WSCC System

4.1 Large system considerations

An important aspect of any new approach to security is to validate the methodology on practical large systems. This section investigates the margin estimation on the WSCC system. The WSCC provides the coordination of power system for the western part of the continental United States, Canada, and Mexico. The WSCC region encompasses approximately 1.8 million square miles, representing a service area equivalent to more than one-half of the contiguous area of the United States. The WSCC system contains more than 5000 buses in the standard operations model used here. For a system of this size and complexity, there are a few assumptions needed to facilitate the study. Primarily, the studies have assumed typical generation patterns during peak and off-peak load conditions. Further, only major contingencies are analyzed and the overall system topology does not vary greatly as it does from season to season as units undergo maintenance.

Due to the vastness and diverse characteristics of the region, WSCC's members face unique challenges in coordinating the day-to-day interconnected system operation and the long-range planning needed to provide reliable and affordable electric service to more than 65 million people in WSCC's service territory. COI (California Oregon Intertie) and PDCI (Pacific Direct Circuit Intertie) are the key transfer paths between Pacific Northwest and California & Nevada. In winter, power transfers from south to north, in summer, power goes from north to south. The impact of various transfers and the COI on margins is studied since transfer on key paths is known to impact margins significantly. Some insight to the critical paths can be gleaned from [54, 55] that serves as a useful guide for our approach. The relations between these critical paths and the COI/PDCI are usually plotted as nomograms but nomograms are limited to a one-to-one relationship. With such a simplified view of system conditions, the operator is unable to have a complete understanding of operational limits. Conceptually, the pattern matching approach factors in different operating conditions into the nomogram approach so operators have a more complete system view.

4.2 Modified neural network approach

In this section, the neural network approach developed in section 3 is refined as appropriate for the WSCC. There are five main considerations:

(1) Feature selection
There are three kinds of input features: real power flow, reactive power loss and reactive power reserve. This information is needed to consider both kinds of voltage instability: “loss of voltage control” voltage instability and “clogging voltage instability”. The first kind of instability is caused by exhaustion of reactive supply with resultant loss of voltage control on a particular set of generators, synchronous condensers, or SVC’s. The loss of voltage control not only cuts off the reactive supply to a subregion requiring reactive power, but also increases reactive network losses that prevent sufficient reactive supply from reaching the subregion needing reactive power. The second kind instability occurs due to I^2X series reactive losses, tap changers reaching tap limits, switchable shunt capacitors reaching susceptance limits, and shunt capacitive withdrawal due to decreasing voltage. The network reactive losses that result from the above

possibilities can choke off the reactive flow to a subregion needing reactive supply without any exhaustion of reactive reserves and loss of voltage control on generators, synchronous condensers, or SVC's. For WSCC system, we select features based on engineering knowledge and correlation coefficients from security studies. Again, [54, 55] provide a good source for real power flow selections. Correlation information is used for all three kinds of features.

(2) Principal component analysis
Principal component analysis provides a mapping from data space to feature space. The first step provided 43 variables as likely inputs to the neural network for P margin estimation on California and Nevada area load. Using principal component analysis, these inputs can be trimmed to 19, which greatly reduces the size of network and the time for training. In the COI transfer P margin estimation, the number of input is reduced from 106 to 46. The accuracy is also improved due to the orthogonality of the data; i.e., the elimination of unnecessary data.

(3) Two hidden layers
With only one hidden layer, the neurons tend to interact with each other globally. In complex situations, these interactions make it difficult to improve the approximation at one point without worsening it at some other points. On the other hand, with two hidden layers the approximation process becomes more manageable. The local features are extracted in the first hidden layer, and global features are extracted in the second hidden layer. The results also show that it reduces the training time while increasing the accuracy.

(4) Determination of network size
It is desirable to determine the optimal regularization parameters in an automated fashion. One approach to this process is the Bayesian framework of David MacKay [56]. In this framework, the weights and biases of the network are assumed to be random variables with specified distributions. The regularization parameters are related to the unknown variances associated with these distributions. The parameters are then estimated using statistical techniques. Bayesian regularization is implemented in Matlab. For the developed network, Bayesian regularization is used first, then the neural networks with the optimum parameters are trained using the Levenberg-Marquardt algorithm.

(5) Splitting training data for estimation and validation
A statistical theory of the overfitting phenomenon is presented in [57]. In nonasymptotic mode, for which N<W, where N is the size of the training set and W is the number of free parameters in the network, there is practical merit in the use of cross-validation to stop training. The optimum value of parameter *r* that determines the split of the training data between estimation and validation subsets is defined by

$$r_{opt} = 1 - \frac{\sqrt{2w-1}-1}{2(w-1)} \tag{4.1}$$

In the developed network, W is around 200, so r_{opt}=0.95, that is, 5% of the training data is used for validation.

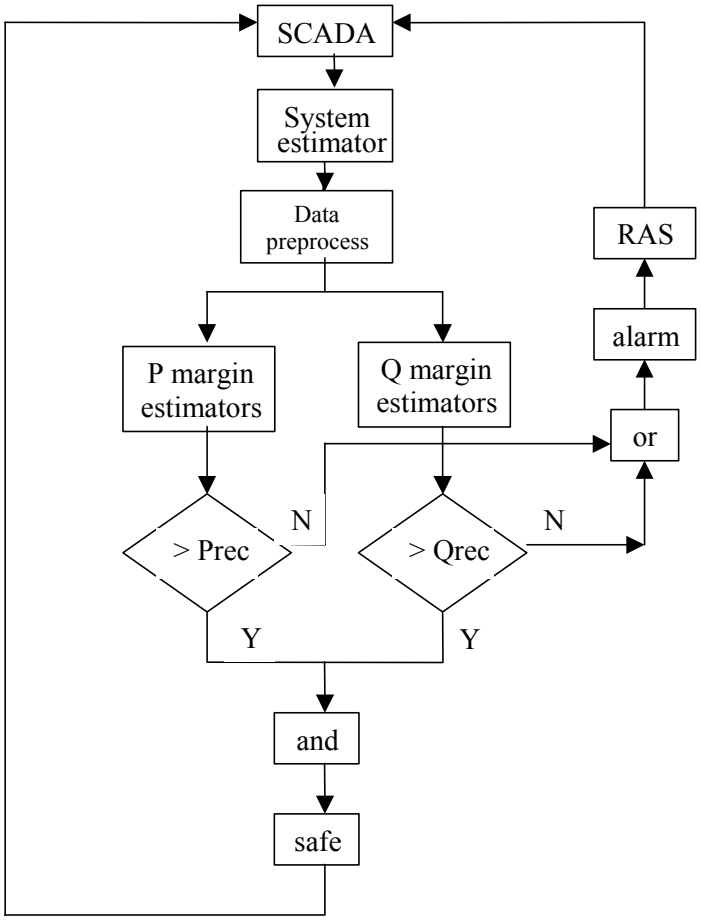

Figure 4.1 System diagram using neural network margin estimators

4.3 Comprehensive method for VSA

The overall approach to determining the voltage security is depicted in Figure 4.1. The input of the neural network voltage stability margin comes from the state estimator. After preprocessing, (extracting critical paths, zone reactive power reserve and reactive power losses), the data would be fed into the neural network. Then principal component analysis is used to further process the data. This data will be presented to pre-trained neural networks specific to different security indicators. Different neural networks are introduced to improve overall robustness of the approach and act as form of fault tolerance. As depicted in Figure 4.2, each of the different margin estimators is independent. These networks may have entirely different structures and may be trained on different sets of data. The lowest and highest estimates are disregarded and the remaining estimates are averages. Limit checks are applied to the outputs to ensure security margins are maintained.

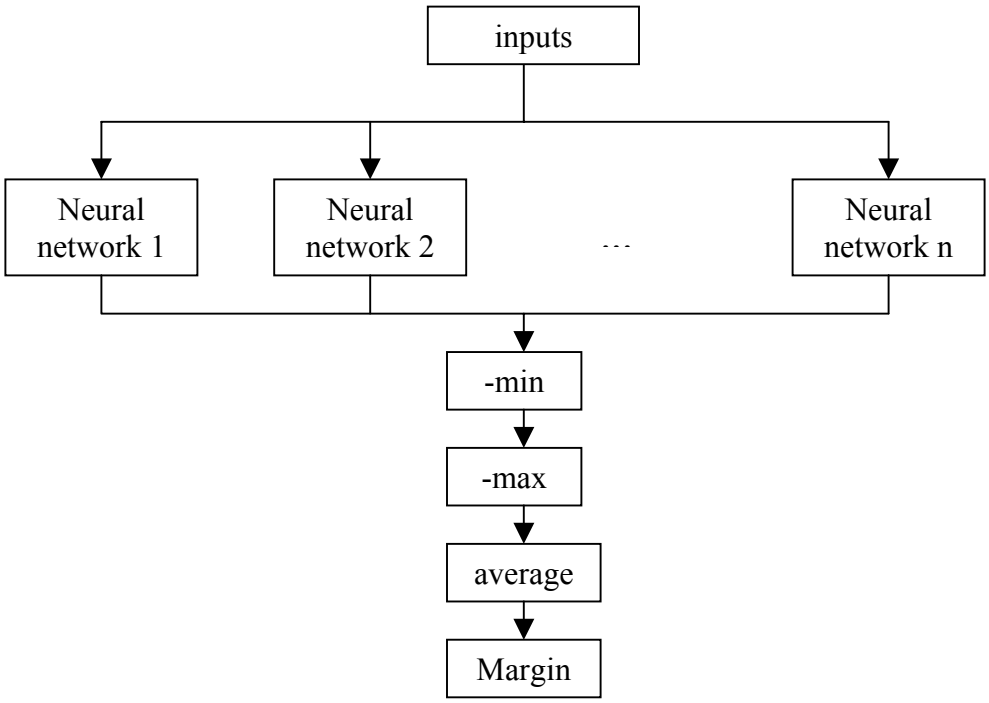

Figure 4.2 Margin estimator structure

4.4 Numerical results

4.4.1 System description

The training and testing data comes from the traditional PV method computations. WSCC system model has more than 5000 buses, 22 areas, 96 zones and more than 1000 generating units. In the first set of the test, our focus is on the following areas: BC Hydro, Pacific Northwest, Montana, PG&E, LADWP, Nevada, San Diego, and Southern California. In the next, our focus is on the COI transfer.

4.4.2 P margin estimation in California and Nevada area

The networks are first applied to the P margin estimation of California and Nevada area load. The study scenario begins with the winter flows, where the flow on COI is from south to north, load is then gradually increased in the PG&E, LADWP, Nevada, San Diego and Southern California areas, which have similar weather patterns. The increased load will be served by dispatching the generation units in BC Hydro, Northwest and Montana, thus, incrementally reaching the typical summer flows from North to South. The security margin will decrease gradually as this transfer increases. The total load in South in the base case is 35,489 MW. The step size is around 1200 MW. There are totally five cases. The maximum load is 40,289 MW. For each load level, all n-1 contingencies of lines above 345 KV and some 230 KV are studied (354 different contingencies) so the number of studies is 1775. For all these cases, power margins are computed and the operating data for the selected features are recorded.

Engineering knowledge is first used to select feature candidates. Then correlation coefficients are computed to get better information about feature selection. The correlations between the 175 inputs and P margin are listed in Table 4.1. The features are selected from this sorted table based on correlation coefficient and some engineering judgement. There are 32 features come from real power flows and 9 from reactive power losses (the selected features are denoted by *). These features include power flows on significant paths such as Canadian Intertie between BCHA and BPA, COI, Midpoint-Summer lake, and so on. These selected features are the inputs to neural networks. Next, several neural networks with different sizes (near to the optimum size as computed by Bayesian regularization) are investigated. The results are listed in Table 4.2 where numbers are in MW. The P margin is the total of areas including PG&E, LADWP, Nevada, San Diego and Southern California. The statistical data of the performance of the neural networks is listed in Table 4.3.

Table 4.1 Correlation coefficients between line flow information and P margin (only the largest and smallest correlations are shown here)

Real power flow index	Correlation coefficient	Reactive power flow index	Correlation coefficient	Reactive power loss index	Correlation coefficient
42*	-0.9544	91	-0.9127	1*	-0.9255
95*	-0.9517	10	-0.886	64*	-0.9071
12*	-0.949	11	-0.8573	65*	-0.9071
27*	-0.9483	93	-0.844	33*	-0.8937
21*	-0.9422	94	-0.844	31*	-0.8333
35*	-0.942	19	-0.8063	135	-0.7481
26*	-0.9415	20	-0.8049	136	-0.7191
25*	-0.9409	43	-0.7997	8	-0.7126
9*	-0.9378	80	-0.798	79	-0.6674
39*	-0.9351	6	-0.7615	17	-0.6217
40*	-0.9351	135	-0.7068	18	-0.6214
41*	-0.9321	136	-0.6358	16	-0.6059
72*	-0.9153	121	-0.6149	71	-0.5583
48*	-0.9099	49	-0.5838	83	-0.5362
5*	-0.9014	3	-0.5712	48	-0.4871
97	-0.8868	71	-0.538	157	-0.4836
38	-0.8836	34	-0.5297	156	-0.4836
16	-0.8821	7	-0.5241	130	-0.4669
32	-0.8769	139	-0.4821	3	-0.4482
33*	-0.8759	134	-0.4792	86	-0.4423
37	-0.8703	4	-0.4721	32	-0.4217
36	-0.8691	64	-0.419	4	-0.4057
153	-0.8293	65	-0.419	144	-0.4049
86	-0.8284	78	-0.404	138	-0.3952
152	-0.8279	24	-0.4037	67	-0.3812
67	-0.8252	149	-0.3842	49	-0.2706
91*	-0.814	102	-0.3798	127	-0.2678
7*	-0.8081	22	-0.3656	145	-0.2623

Table 4.1 Correlation coefficients between line flow information and P margin (cont.)

103	-0.7764	57	-0.3603	112	-0.2612
46	-0.7737	56	-0.3603	134	-0.2398
47	-0.7677	53	-0.3314	160	-0.1549
127	-0.7409	69	-0.3123	26	-0.1409
49	-0.732	147	-0.3005	25	-0.1402
…	…	…	…	…	…
6	0.7969	86	0.4356	24	0.405
24	0.7973	157	0.4358	139	0.4056
80	0.8171	156	0.4358	12	0.4183
79	0.8336	8	0.4435	154	0.5052
77	0.8587	9	0.474	97	0.5407
156	0.8691	21	0.4849	53	0.5439
157	0.8691	54	0.4909	61	0.544
43	0.8881	62	0.5046	99	0.5752
20	0.8892	79	0.5495	35	0.5916
19	0.8894	99	0.5523	6	0.6337
70	0.8964	92	0.5576	142	0.6391
10	0.8968	35	0.5865	149	0.6467
11*	0.9011	63	0.601	42	0.7185
1*	0.9012	39	0.6034	121	0.7283
34*	0.9194	40	0.6034	72	0.7283
123*	0.9229	77	0.6111	41	0.7696
136*	0.9259	25	0.6421	2	0.7955
129*	0.9308	67	0.6511	22	0.7956
112*	0.9336	103	0.6531	129	0.8417
135*	0.938	26	0.6656	21	0.8429
99*	0.9525	138	0.7094	11	0.861
31*	0.955	142	0.7388	77	0.8621
83*	0.9578	5	0.7806	20	0.8777
63*	0.9652	33	0.7906	19	0.8779
64*	0.9652	83	0.8073	91*	0.9065
65*	0.9652	16	0.8192	7*	0.9174
93*	0.9653	95	0.8193	93*	0.9564
94*	0.9653	27	0.8454	94*	0.9564

Table 4.2 The estimation of P margin of California using 5 different networks

Network 1		Network 2		Network 3		Network 4		Network 5	
label	estimation	label	estimation	label	estimation	label	estimation	label	estimation
3.3000	3.2896	7.8000	7.7830	3.3000	3.3433	3.3000	3.3086	5.7000	5.6506
7.8000	8.0476	8.1000	8.0686	6.9000	6.8787	8.1000	8.0868	3.3000	3.2899
8.1000	8.0745	8.1000	8.0732	4.8000	4.8263	4.5000	4.4431	3.3000	3.2998
8.1000	8.0777	8.1000	8.0509	4.5000	4.4840	4.2000	4.0566	6.9000	6.8609
5.7000	5.6629	4.5000	4.5180	6.9000	6.8815	6.9000	6.9186	5.7000	5.7022
8.1000	8.0694	5.7000	5.5236	6.9000	6.8766	8.1000	8.0693	6.9000	6.8898
8.1000	8.0647	3.3000	3.3058	3.3000	3.3019	4.5000	4.4650	3.3000	3.2976

Table 4.2 The estimation of P margin of California using 5 different networks (cont.)

6.9000 6.9180	3.3000 3.2093	4.2000 4.2035	8.1000 8.1039	4.5000 4.4774
5.7000 5.7083	6.9000 7.0097	8.1000 8.0567	5.7000 5.7063	3.3000 3.2410
3.3000 3.3496	5.7000 5.7068	8.1000 8.0618	5.4000 4.7745	6.9000 6.9484
6.9000 6.8633	8.1000 8.1277	6.6000 6.5680	8.1000 8.0790	4.5000 4.4324
8.1000 8.0830	4.5000 4.4709	6.9000 6.8737	4.5000 4.4068	4.5000 4.5155
5.7000 5.6565	8.1000 8.0709	5.7000 5.6950	5.7000 5.5936	6.9000 6.7056
3.3000 3.2722	6.9000 6.8656	3.3000 3.3955	5.7000 5.6970	4.5000 4.4815
6.9000 6.8819	3.3000 3.2764	5.7000 5.6725	3.3000 3.2936	5.7000 5.7030
5.4000 5.3988	4.5000 4.4859	4.5000 4.4668	8.1000 8.0853	8.1000 8.0970
8.1000 8.0764	5.7000 5.7183	8.1000 8.0766	5.7000 5.7015	3.3000 3.3052
4.5000 4.5205	6.6000 6.6760	4.5000 4.4522	5.4000 5.2171	4.5000 4.4469
7.8000 8.1550	5.7000 5.7009	3.3000 3.2817	7.8000 8.0427	3.3000 3.2886
5.7000 5.7386	6.9000 6.8941	4.5000 4.4517	6.9000 6.9318	3.3000 3.3024
3.3000 3.2626	4.2000 4.0576	3.3000 3.3041	8.1000 8.0922	3.3000 3.1240
6.9000 6.8821	6.9000 6.8815	6.9000 6.8864	5.7000 5.6283	4.5000 4.4801
5.7000 5.6353	7.8000 7.8667	3.3000 3.2844	4.5000 4.4402	3.3000 3.2735
6.9000 6.8850	6.9000 6.8555	6.9000 6.8813	4.5000 4.3933	5.7000 5.6863
5.7000 5.7295	3.0000 2.8914	6.9000 6.9399	5.7000 5.6195	3.0000 2.7980
6.9000 6.9121	3.3000 3.3374	6.9000 7.0383	8.1000 8.0911	2.7000 3.0453
8.1000 8.0756	4.4036 4.5033	3.3000 3.2907	5.7000 5.6975	3.3000 3.3018
8.1000 8.0847	5.7000 5.7222	8.1000 8.0672	3.3000 3.3069	3.3000 3.4093
3.3000 3.2382	6.9000 6.9160	4.5000 4.4686	8.1000 8.0933	4.5000 4.5652
3.3000 3.2400	4.5000 4.4648	5.7000 5.7034	7.5000 7.4946	8.1000 8.0949
3.3000 3.2933	4.5000 4.4742	8.1000 8.0397	3.3000 3.2914	5.7000 5.6924
4.5000 4.4692	6.9000 6.8910	5.7000 5.6951	8.1000 8.0898	5.7000 5.7678
8.1000 8.0953	3.0000 2.9714	4.5000 4.4694	8.1000 8.1182	6.9000 6.8650
3.0000 3.1153	5.7000 5.7071	5.7000 5.6749	8.1000 8.0849	4.5000 4.4962
6.9000 6.8738	6.6000 6.7604	8.1000 8.0609	5.7000 5.7130	6.9000 6.8439
5.7000 5.6676	8.1000 8.0746	3.3000 3.2412	6.9000 6.8920	5.7000 5.6941
8.1000 8.1036	6.9000 6.8038	6.9000 6.8808	8.1000 8.1071	5.7000 5.6990
6.9000 6.8680	5.7000 5.7154	4.5000 4.4397	5.7000 5.7137	3.9000 4.4707
6.9000 6.7659	8.1000 8.0733	6.9000 6.8783	5.7000 5.6991	3.3000 3.2964
2.7000 2.8769	6.9000 6.8795	4.5000 4.4781	3.3000 3.0640	4.5000 4.5044
8.1000 8.0666	4.5000 4.4733	6.9000 6.8671	6.9000 6.8966	8.1000 8.1269
4.5000 4.5671	3.3000 3.3046	8.1000 7.7916	3.3000 3.2913	4.5000 4.5032
6.9000 6.8318	3.3000 3.3248	6.9000 6.9348	3.3000 3.2933	3.3000 3.3034
4.5000 4.4763	4.5000 4.4752	5.7000 5.6859	8.1000 8.0868	8.1000 7.8859
7.8000 8.2037	4.5000 4.4637	8.1000 8.0603	6.9000 6.7912	8.1000 8.0963
3.3000 3.2981	3.3000 3.3426	3.3000 3.2804	4.5000 4.4820	4.5000 4.4885
6.9000 6.9181	5.7000 5.7298	3.3000 3.2932	6.9000 6.8966	6.9000 6.8835
6.9000 6.8588	6.9000 6.8834	5.7000 5.6938	4.5000 4.4950	4.5000 4.4959
3.3000 3.3162	5.1000 4.9011	4.5000 4.4720	3.0000 3.1084	6.9000 6.8038
5.7000 5.7007	6.9000 6.8791	8.1000 8.0613	5.7000 5.7153	6.6000 7.0033
8.1000 8.0832	5.4000 5.2948	8.1000 8.0577	8.1000 8.0885	5.7000 5.7032
3.3000 3.3056	6.9000 6.8665	4.5000 4.4501	6.9000 6.8772	6.9000 6.8802

Table 4.2 The estimation of P margin of California using 5 different networks (cont.)

5.4000 5.5130	8.1000 8.0754	3.3000 3.5320	4.5000 4.5012	5.7000 5.6929
6.9000 6.8595	4.5000 4.4746	4.5000 4.4840	4.5000 4.4964	3.3000 3.2978
6.9000 6.8410	5.7000 5.7000	3.3000 3.2902	7.8000 8.0002	5.7000 5.6868
6.9000 6.8669	5.7000 5.7250	5.4000 5.3202	4.5000 4.4918	4.5000 4.2688
8.1000 8.0732	3.3000 3.3246	8.1000 8.0686	4.5000 4.4873	8.1000 8.1049
3.3000 3.2909	8.1000 8.0716	4.5000 4.4659	6.9000 6.9632	6.9000 6.9124
5.1000 5.1168	4.2000 4.4371	6.6000 6.8631	4.5000 4.5484	5.7000 5.6963
6.9000 6.8721	5.7000 5.7049	5.7000 5.6342	3.3000 3.3087	6.9000 6.8999
8.1000 8.0700	5.7000 5.7248	8.1000 8.0581	4.5000 4.4951	8.1000 8.0979
3.3000 3.2918	8.1000 8.2023	6.9000 6.8892	8.1000 8.0702	3.3000 3.2961
5.7000 5.6858	3.0000 3.2634	5.7000 5.6752	7.5000 8.0724	4.5000 4.5074
4.5000 4.5148	4.5000 4.4409	4.5000 4.4658	5.7000 5.7069	4.5000 4.5050
4.5000 4.4857	8.1000 7.9974	6.9000 6.9298	8.1000 8.1000	3.3000 3.3325
4.5000 4.4851	3.3000 3.3842	6.9000 6.8717	4.2000 4.3022	4.5000 4.4187
3.3000 3.3097	8.1000 8.0738	8.1000 8.0584	6.9000 6.8882	6.9000 6.8765
3.3000 3.3694	6.9000 6.8691	6.9000 6.8514	4.5000 4.4964	5.7000 5.7018
4.5000 4.4719	8.1000 8.0721	4.5000 4.4500	3.3000 3.3001	3.3000 3.2982
3.3000 3.2755	8.1000 7.9415	4.5000 4.4737	3.3000 3.0790	6.9000 6.8779
4.5000 4.4749	5.4000 5.3120	7.8000 7.7290	6.9000 6.9088	5.7000 5.6976
4.5000 4.4625	5.7000 5.7097	5.7000 5.6799	8.1000 8.0872	3.3000 3.2394
4.5000 4.4758	4.5000 4.4923	4.8000 5.4833	3.3000 3.2937	5.7000 5.6986
3.3000 3.1904	4.2000 3.6133	8.1000 8.1366	3.3000 3.2905	8.1000 8.0632
6.9000 6.8943	4.5000 4.4361	5.7000 5.7030	8.1000 8.3106	3.6000 3.4757
6.9000 6.8617	4.5000 4.4362	8.1000 8.0251	4.2000 4.0067	5.7000 5.6936
8.1000 8.1039	5.7000 5.7224	6.9000 6.8345	3.3000 3.2949	4.5000 4.4979
3.3000 3.2872	5.7000 5.8284	4.2000 4.4552	5.7000 5.6989	6.9000 6.8901
3.3000 3.2925	3.3000 3.3868	4.5000 4.4433	4.5000 4.4919	4.5000 4.4878
6.6000 6.6950	3.3000 3.3354	4.5000 4.4653	5.7000 5.5978	6.9000 6.8773
6.9000 6.9348	6.9000 6.8824	5.7000 5.6813	6.9000 6.8815	5.7000 5.7021
8.1000 8.1025	5.7000 5.6746	7.5000 8.0479	3.3000 3.3111	6.9000 6.9868
3.3000 3.2917	8.1000 8.0278	3.0000 2.9252	3.3000 3.3742	4.5000 4.5487
4.2000 4.1375	5.7000 5.7075	5.7000 5.6691	6.9000 6.9181	3.3000 3.2763
8.1000 8.0668	4.5000 4.4359	5.7000 5.7200	8.1000 8.0763	8.1000 8.0784
5.7000 5.6399	8.1000 8.0729	6.9000 6.8644	5.7000 5.6437	8.1000 7.9819
4.5000 4.4851	5.7000 5.7142	8.1000 8.0593	5.7000 5.6921	6.9000 6.8683
8.1000 8.0787	3.3000 3.3033	8.1000 8.0611	5.7000 5.6020	5.7000 5.6977
8.1000 8.0830	6.9000 6.7279	8.1000 8.0088	6.9000 6.9095	4.5000 4.4749
6.9000 6.8586	6.9000 6.8654	6.9000 6.8748	8.1000 8.0777	4.5000 4.4655
3.3000 3.2919	4.5000 4.4815	8.1000 8.0611	3.0000 3.2896	6.9000 6.8668
6.6000 6.5865	5.7000 5.7099	4.5000 4.4707	6.9000 6.8814	8.1000 8.0617
5.7000 5.6945	5.7000 5.7132	4.5000 4.4811	8.1000 8.0677	3.3000 3.3145
3.3000 3.2956	4.5000 4.4736	4.5000 4.4531	3.0000 2.9163	3.3000 3.2913
4.5000 4.4835	2.7000 2.6228	6.9000 6.9518	4.2000 4.0912	3.3000 3.2993
3.0000 3.1464	5.7000 5.7746	3.2036 3.3198	8.1000 8.0937	6.9000 6.8828
4.5000 4.4629	3.3000 3.3108	3.3000 3.2773	5.7000 5.6565	4.2000 4.1804

Table 4.2 The estimation of P margin of California using 5 different networks (cont.)

8.1000 8.0688	4.5000 4.5018	4.5000 4.4735	8.1000 7.8278	5.7000 5.6826
8.1000 8.0854	1.2000 1.0488	8.1000 8.0617	5.4000 5.3513	5.7000 5.6832
8.1000 8.0926	6.9000 6.8327	6.9000 6.8707	3.0000 3.0432	4.5000 4.5060
4.5000 4.4988	4.5000 4.4866	6.9000 6.9622	4.5000 4.4832	5.7000 5.7031
6.6000 6.6960	6.9000 6.8756	6.9000 6.8850	3.3000 3.2920	3.3000 3.3012
6.9000 7.0576	6.9000 6.8764	6.9000 6.8706	3.3000 3.2782	3.9000 4.1020
7.2000 6.7310	5.7000 5.7274	6.9000 6.8844	5.4000 5.3628	5.7000 5.6224
6.9000 6.8527	4.2000 4.2373	4.5000 4.5055	4.5000 4.4695	6.9000 6.8909
3.3000 3.2909	5.7000 5.7090	7.8000 7.4447	6.6000 6.7304	6.9000 6.8809
4.5000 4.4858	4.5000 4.4963	6.9000 6.8713	3.3000 3.3514	1.2000 1.1562
6.9000 6.8721	3.3000 3.3038	4.5000 4.4600	3.3000 3.3381	5.7000 5.6392
5.7000 5.6791	5.7000 5.5647	3.3000 3.2793	8.1000 8.0770	4.5000 4.5049
6.6000 6.6185	5.7000 5.7040	6.9000 6.8988	4.5000 4.4810	6.6000 6.6995
8.1000 8.0680	8.1000 8.0855	6.9000 6.8720	3.3000 3.3012	4.5000 4.4921
8.1000 8.0875	4.2000 4.4161	6.6000 6.9117	3.3000 3.2618	6.9000 6.8790
6.9000 6.8316	8.1000 7.9807	3.3000 3.2831	3.3000 3.2627	3.3000 3.2972
6.9000 6.8050	3.3000 3.3236	6.9000 6.8785	4.5000 4.5023	4.5000 4.4559
8.1000 8.0759	6.9000 6.8745	6.9000 6.8628	6.9000 6.8927	5.7000 5.6721
6.6000 6.8364	6.9000 6.8660	6.9000 6.8624	4.5000 4.4741	5.7000 5.6883
8.1000 8.0706	6.9000 6.8914	6.9000 6.8837	3.3000 3.3084	4.5000 4.4834
3.3000 3.3005	3.3000 3.6947	5.7000 5.6799	3.3000 3.4456	4.5000 4.4979
6.9000 6.8650	5.1000 5.5807	5.7000 5.6966	3.3000 3.2927	5.7000 5.6818
4.5000 4.4629	5.7000 5.7109	8.1000 8.0797	3.3000 3.2764	6.9000 6.8949
8.1000 8.0846	3.3000 3.3007	4.5000 4.4127	5.7000 5.6642	3.2036 3.3236
8.1000 8.0790	4.5000 4.4858	6.9000 6.8970	6.9000 6.8909	6.6000 6.5531
5.7000 5.7115	6.9000 6.8729	3.3000 3.2820	3.3000 3.1703	3.3000 3.2837
8.1000 8.0450	8.1000 8.0786	6.9000 6.8804	5.4000 5.4307	5.7000 5.6642
8.1000 8.0915	6.9000 7.0276	5.7000 5.7128	3.3000 3.2867	3.3000 3.3020
8.1000 8.0802	7.8000 7.9717	6.9000 6.8863	6.9000 6.8771	3.3000 3.2948
3.3000 3.2895	5.7000 5.6972	3.3000 3.2976	4.5000 4.5210	4.5000 4.5775
4.5000 4.4808	5.7000 5.7657	8.1000 8.0649	4.5000 4.4832	5.7000 5.6584
4.5000 4.4739	6.9000 6.8665	3.3000 3.2835	5.7000 5.7698	6.9000 6.8714
6.9000 6.8761	8.1000 8.0865	8.1000 8.0673	5.7000 5.6837	6.6000 6.9055
4.5000 4.4603	3.2036 3.3402	5.7000 5.5600	6.9000 6.8830	8.1000 8.0807
8.1000 8.3451	5.4000 5.5278	3.3000 3.3305	3.3000 3.2915	8.1000 8.0969
6.9000 6.8656	8.1000 7.9822	8.1000 8.0508	4.5000 4.4998	4.5000 4.4798
5.7000 5.6745	6.9000 6.8763	5.7000 5.6770	6.9000 6.8852	6.9000 6.9392
4.5000 4.4669	8.1000 8.0746	3.3000 3.2713	6.9000 6.8823	4.5000 4.3435
5.7000 5.6816	4.5000 4.4972	3.3000 3.2930	4.5000 4.4789	5.7000 5.7021
3.3000 3.3025	4.5000 4.5098	8.0036 8.0804	5.7000 5.7455	5.7000 5.6987
3.3000 3.2721	8.1000 8.0714	5.1000 5.3486	6.9000 6.8650	6.9000 6.9405
4.4036 4.5064	3.3000 3.3207	5.7000 5.6787	7.8000 7.7946	5.7000 5.6140
6.9000 6.8699	8.1000 8.0223	5.7000 5.6735	5.7000 5.6943	4.5000 4.5060
5.7000 5.7086	5.7000 5.7101	3.3000 3.2840	6.9000 6.9416	3.3000 3.2653
4.5000 4.4957	7.2000 8.0823	5.4000 5.5534	6.9000 6.9023	8.1000 8.1019

Table 4.2 The estimation of P margin of California using 5 different networks (cont.)

4.8000 5.7039	5.7000 5.7270	4.5000 4.4471	5.7000 5.7204	4.5000 4.4650
6.9000 6.8776	8.1000 8.0702	5.7000 5.6935	5.7000 5.6954	4.5000 4.4996
8.1000 8.0501	4.2000 4.3828	5.7000 5.7075	8.1000 8.0812	4.5000 4.4945
6.6000 6.5827	6.9000 6.8954	5.7000 5.6770	6.9000 6.8920	5.7000 5.7547
8.1000 8.0795	6.9000 6.8854	5.7000 5.7218	6.9000 6.8988	6.9000 6.9054
3.3000 3.2941	5.1000 5.5000	6.9000 6.8633	8.1000 8.0912	3.3000 3.3115
6.9000 6.8686	3.3000 3.3384	7.8000 7.7915	8.1000 8.0381	6.9000 6.8766
8.1000 8.0478	5.7000 5.7175	4.5000 4.4396	6.9000 6.8922	7.8000 7.7403
8.1000 8.0943	4.5000 4.4755	8.1000 8.0678	8.1000 8.0741	5.7000 5.6977
4.5000 4.4930	4.2000 4.2997	4.5000 4.4578	6.9000 6.8770	5.4000 5.3366
4.5000 4.5034	3.3000 3.3104	6.3000 6.3959	4.5000 4.4763	3.3000 3.2806
4.5000 4.4487	4.5000 4.4565	3.3000 3.2847	5.7000 5.7052	6.9000 6.8887
4.5000 4.4812	7.8000 8.2935	4.5000 4.4594	6.9000 6.8907	5.4000 5.3211
8.1000 8.0748	4.5000 4.4858	4.5000 4.4366	4.2000 4.2351	6.9000 6.8932
6.9000 6.8982	6.9000 6.8654	7.8000 6.9082	4.5000 4.4205	3.3000 3.2941
6.9000 6.8849	7.5000 8.0701	6.9000 6.9815	4.5000 4.5198	4.5000 4.5033
8.1000 8.0831	8.1000 8.0826	6.9000 6.8793	4.5000 4.5314	6.9000 6.8858
5.7000 5.7085	8.1000 8.0765	5.7000 5.6971	3.3000 3.2814	3.3000 3.3190
3.3000 3.2924	8.1000 8.1118	2.7000 2.7802	8.1000 8.0759	5.7000 5.6150
3.3000 3.2924	5.7000 5.7178	8.1000 7.9913	3.3000 3.2931	3.3000 3.3040
3.3000 3.4829	6.9000 6.8845	3.3000 3.6162	5.7000 5.6859	3.3000 3.2586
6.9000 6.8748	5.7000 5.4380	5.7000 5.7595	5.7000 5.6804	5.7000 5.6959
5.4000 5.3750	4.5000 4.4878	8.1000 8.0823	3.3000 3.3581	6.9000 6.8912
4.5000 4.4488	3.3000 3.3025	6.9000 6.8933	6.9000 6.8912	3.0000 2.9210
8.1000 7.9038	5.7000 5.4650	8.1000 8.0566	3.3000 3.2895	4.5000 4.3463
3.3000 3.2813	8.1000 8.0720	8.1000 8.0614	6.9000 6.8817	4.5000 4.5001
8.1000 8.0812	6.9000 6.8815	5.7000 5.6662	4.5000 4.5057	6.3000 6.4694
3.3000 3.2694	8.1000 8.0370	4.5000 4.5393	5.7000 5.7141	8.1000 7.8419
8.1000 8.1118	4.5000 4.4923	5.7000 5.7664	3.3000 3.2927	4.5000 4.5050
4.2000 4.3037	8.1000 8.0717	5.1000 5.3700	4.5000 4.5106	8.1000 8.0208
8.1000 8.2186	8.1000 8.0577	4.5000 4.4823	6.3000 6.6988	6.0000 6.7772
4.5000 4.4851	3.3000 3.3184	5.7000 5.6618	5.7000 5.6888	3.3000 3.3601
4.5000 4.4485	3.3000 3.3167	4.5000 4.4538	5.4000 5.6440	4.5000 4.5837
4.5000 4.4804	3.3000 3.3383	8.1000 8.0798	4.5000 4.4833	5.7000 5.6964
4.2000 3.9404	8.1000 8.0826	3.3000 3.2937	4.5000 4.5164	5.7000 5.7051
5.7000 5.6934	5.7000 5.6064	3.3000 3.2800	4.5000 4.4941	3.3000 3.2959

Table 4.3: The performance of networks on California load margin estimation

	Network 1	Network 2	Network 3	Network 4	Network 5
Number of hidden neuron(1^{st}+2^{nd} layer)	7+4	7+3	6+4	8+3	8+4
Max error(MW)	904.00	882.3	891.8	625.5	777.2
Mean error(MW)	105.21	133.20	121.39	97.62	104.24
Standard deviation (MW)	105.50	133.40	121.51	97.69	104.51

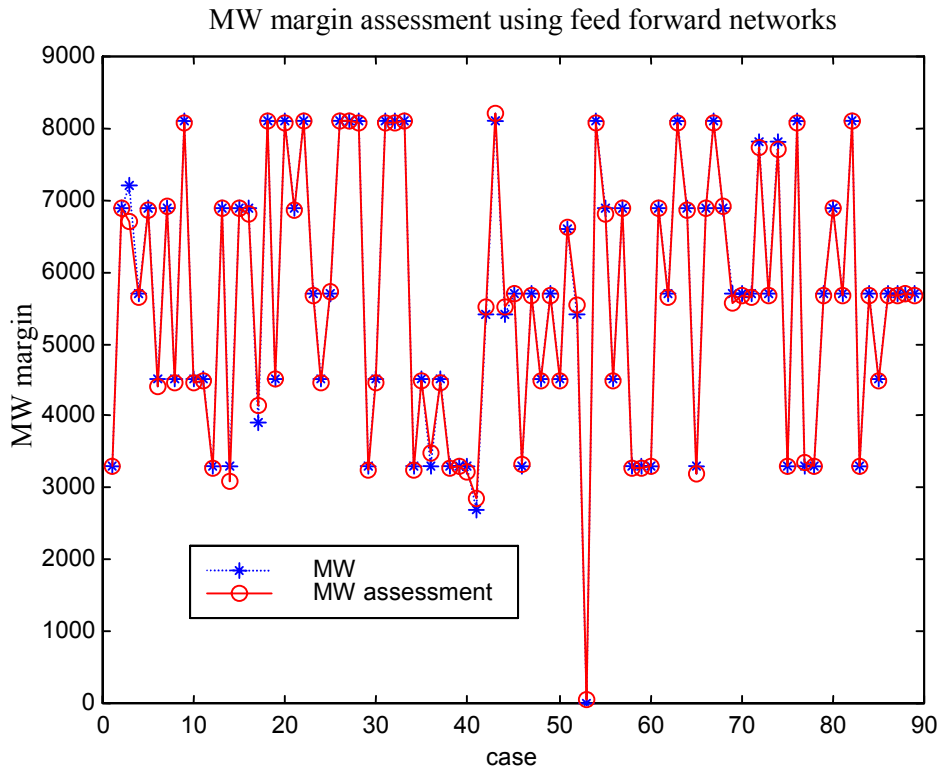

Figure 4.3 The performance of the system model for California load margin

Table 4.4 The performance comparison on the same test data (California load margin)

	Network 1	Network 2	Network 3	Network 4	Network 5	System
Max error (MW)	485.2447	423.6993	396.2494	673.7733	378.7913	420.0951
Mean error (MW)	80.1573	82.3018	89.7667	103.3176	97.2577	74.5145
Standard deviation (MW)	78.8828	82.2095	88.0339	102.8270	95.940	73.5362

Each of the networks is trained and tested with the same data. The overall performance is listed in Table 4.4. The P margin required in these cases is around 2000 MW (P at the nose point of PV curve, 40,000 multiplied by 5% where 5% is defined in WSCC security criteria as performance level A). The last column is the result of system model using a voting mechanism. Note that such a voting mechanism reduces both the mean error and standard deviation. The maximum error (420) of the system is less than the mean (471.55) and median (423.70) maximum error of the 5 individual networks. This is about 21% of the minimum margin requirement. The results are plotted graphically in Figure 4.3. This clearly shows the credibility of the system model for P margin estimation.

4.4.3 P margin estimation over COI transfer limit

The networks are next applied to the P margin estimation for COI transfer limit. First, a new base case is generated which represents a light load in summer (California). Then, gradually the generation is decreased in the California area and the generation is scaled up in the Northwest

and BC Hydro. The effect is to increase the power transfer on COI step by step. There are totally 11 steps until the system could not survive further increase on COI. At each step, the 32 worst n-1 contingencies are studied so the total cases are 336. For each case, P margin on COI transfer, power flows and reactive power losses on major paths and reactive power reserve in interested areas are recorded as training and testing data.

Again, engineering knowledge is first used to select feature candidates. The inputs include real power flow and reactive power loss of some key lines and reactive power reserve in BC Hydro, Northwest, PG&E, Nevada and South California. Then instead of using correlation coefficients, this data is fed to the neural network PREPCA function. As mentioned in section 2, PREPCA can extract useful data and reduce the dimension of the input vectors. It effectively reduced the input number from 106 to 46. The reduced features are the inputs to neural networks. Again, several neural networks with different sizes (close to the optimum size as computed by Bayesian regularization) are tested. The results are listed in Table 4.5. Units in this table are in 1000 MW. The P margin is the margin of transfer on COI. The statistical data on the performance of the neural networks is listed in Table 4.6.

Table 4.5 The estimation of P margin on COI transfer using 5 different networks

network 1		network 2		network 3		network 4		network 5	
label	estimation	label	estimation	label	estimation	label	estimation	label	estimation
0.3728	0.3730	0.2434	0.2330	1.8415	1.7872	0.8523	0.8426	0.1281	0.1385
1.7878	1.7953	1.3843	1.4091	0.0009	-0.0032	0.1281	0.1573	1.0220	1.0744
1.8170	1.8628	1.3613	1.3385	0.3772	0.3740	0.1472	0.1328	0.7019	0.7145
0.5865	0.5821	0.2850	0.2205	0.3308	0.3451	0.7532	0.7437	0.7665	0.7665
0.6929	0.6895	0.2584	0.2491	0.6045	0.5959	0.0758	0.0811	1.3485	1.3126
1.8414	1.8829	0.2042	0.1930	0.2657	0.2609	0.1998	0.2015	0.4876	0.4923
0.5112	0.5073	0.3056	0.3169	0.6605	0.6626	0.3728	0.3885	0.1946	0.1878
0.5156	0.5253	0.3053	0.3386	0.4749	0.4664	0.1219	0.1426	0.0758	0.0391
0.6063	0.6150	0.7102	0.7254	0.5156	0.5174	0.0653	0.0657	0.4204	0.4195
0.0716	0.0964	1.4119	1.4153	0.7102	0.6975	0.9057	0.8972	0.2006	0.1916
0.3988	0.4103	0.2095	0.1973	0.7412	0.7713	0.0573	0.0477	0.7555	0.7569
0.5867	0.6011	1.0614	1.0497	1.1240	1.1339	1.8679	1.8706	0.1638	0.1906
0.0101	0.0092	1.0680	1.0595	0.2799	0.2744	0.4876	0.4929	0.0779	0.0843
0.3673	0.3758	1.8395	1.8414	0.1018	0.0902	0.0244	0.0176	0.5865	0.5914
1.5043	1.5330	1.8414	1.8459	1.8176	1.7322	0.6605	0.6155	0.1472	0.1224
0.9888	1.0094	0.2718	0.2523	0.3840	0.3820	0.9375	0.9630	0.6583	0.6604
0.1899	0.1911	0.6727	0.6826	0.1998	0.1954	0.3058	0.2921	1.2840	1.2522
0.5262	0.4980	0.0244	0.0628	0.5379	0.5413	0.6929	0.7213	0.2452	0.2126
0.7434	0.7279	0.0758	0.0843	0.6029	0.5722	0.0761	0.1111	0.8834	0.8820
0.7575	0.7681	0.6039	0.6017	1.8395	1.8093	1.3421	1.2995	0.9876	0.9969
0.4846	0.4755	0.4060	0.4047	0.0726	0.0624	2.0036	1.8990	0.3058	0.3029
0.5083	0.5028	1.3485	1.3733	0.1486	0.1563	0.5413	0.5439	0.6508	0.6383
0.2806	0.2799	0.1108	0.1118	0.3046	0.2961	0.1919	0.1995	0.0244	0.0252
0.0729	0.0864	0.1254	0.1383	0.9695	0.9554	0.3269	0.3339	0.1298	0.1240
0.4628	0.4514	0.5720	0.5642	0.0244	0.0118	0.7385	0.7310	0.6039	0.5889
0.5413	0.5708	0.1919	0.1845	0.9690	0.9375	0.0257	0.0200	0.1964	0.1918
0.6542	0.6430	0.2378	0.2184	0.3388	0.3371	0.2127	0.2132	1.3856	1.3879

Table 4.5 The estimation of P margin on COI transfer using 5 different networks (cont.)

0.5156	0.4887	0.3771	0.3943	0.0456	0.0445	1.4315	1.4473	0.3046	0.2941
0.4125	0.4100	1.3256	1.2773	1.8484	1.8405	0.0733	0.0448	0.5156	0.5127
1.3426	1.3222	0.0726	0.0745	0.0956	0.1177	0.1376	0.1312	0.3995	0.3989
0.1704	0.2070	0.0786	0.0674	0.1402	0.1302	0.6197	0.6389	0.0399	0.0225
0.3574	0.3621	0.6029	0.6151	1.0680	1.0680	0.2831	0.2863	0.0733	0.0703
0.4749	0.4821	1.8564	1.8920	1.3843	1.3998	0.2952	0.3088	0.5044	0.4764
0.7412	0.7401	0.2042	0.1946	0.3058	0.3042	1.3322	1.3712	0.1472	0.1442

Table 4.6: The performance of networks on COI transfer margin estimation

	Network 1	Network 2	Network 3	Network 4	Network 5
Number of hidden neuron(1^{st}+2^{nd} layer)	16+6	16+5	15+5	15+4	14+3
Max error (MW)	53.48	73.79	63.50	76.24	42.65
Mean error (MW)	20.85	18.77	19.47	24.92	14.72
Standard deviation (MW)	20.68	18.50	19.75	24.35	14.73

Table 4.7 The performance comparison on the same test data (COI transfer margin)

	Network 1	Network 2	Network 3	Network 4	Network 5	System
Max error (MW)	23.45	8.02	32.86	16.64	21.25	7.84
Mean error (MW)	4.07	1.80	7.07	3.03	5.57	1.39
Standard deviation (MW)	4.05	1.77	6.91	3.01	5.63	1.38

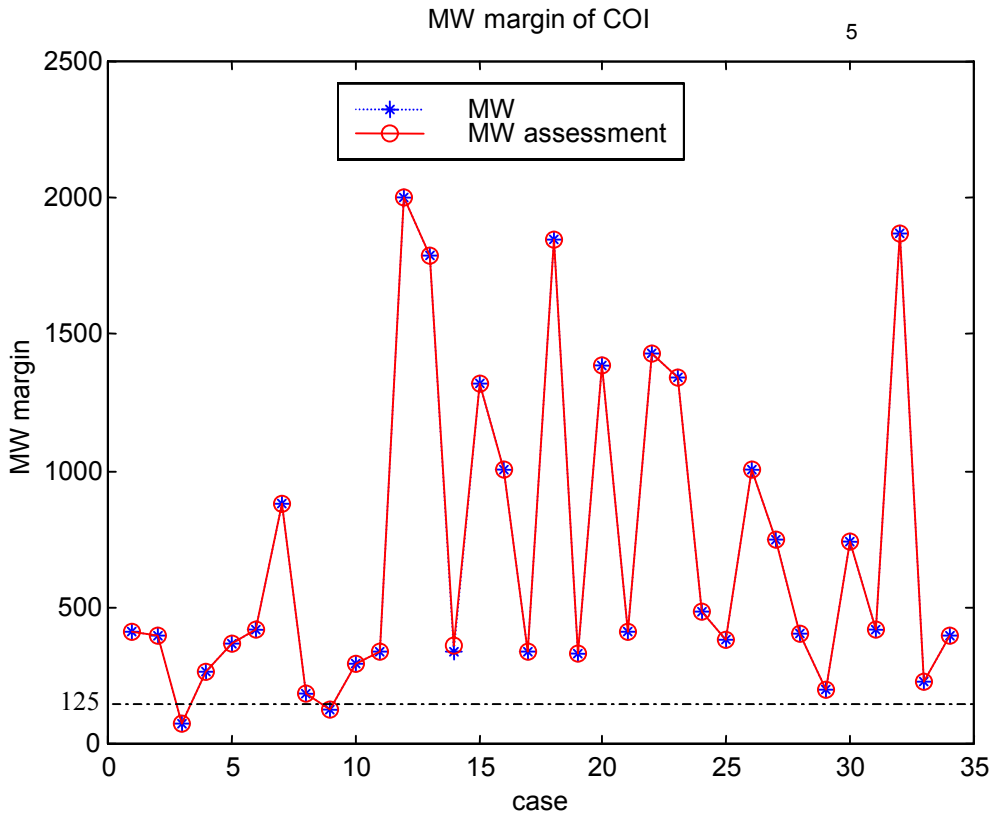

Figure 4.4 The performance of the system model (COI transfer margin)

Again, the networks are fed identical test data. Table 4.7 summarizes the performance. The required P margin on COI is around 125MW (P at the nose point of PV curve, 2500, multiplied by 5% where again 5% is defined in WSCC security criteria as performance level A). The last column is the result of system model using a voting mechanism. Note that using this method decreases the maximum error, mean error and standard deviation. The maximum error is less than 6.3% of the required margin. The result of the system model is plotted in Figure 4.4 showing clearly that the margin is precise for all test cases. This further establishes the credibility of the approach for P margin estimation.

Next two additional cases are studied to show the effect of equipment outages combined with n-1 contingency studies. To begin, the possibility of the outage of the Table Mountain-Tesla 500 kV line in combination with other contingencies is included. The Table Mountain-Tesla line outage will cause a significant decrease in COI transfer limit. The purpose of this study is to test if the neural networks have the ability to generalize under more diverse operating conditions. If so, then a given neural network (or set of five networks in our model) can be used to cover more operating scenarios and in effect act as multiple nomograms. Table 4.8 shows the statistical performance on this data. Figure 4.5 depicts graphically the difference between the estimated and actual margins on this data set. The number of test cases increases here to follow the rule given by equation (4.1). As expected, estimate errors increase. Still, the errors are not large and again, there are no misclassifications. The next set of data adds the possibility of the outage of the Diablo Canyon nuclear unit #1 in combination with other contingencies. Table 4.9 shows the statistical performance on this data. Figure 4.6 depicts graphically the difference between the estimated and actual margins on this data set. Again, the errors are not large and there are no misclassifications. This provides further justification of the use of these networks for widely varying system conditions.

Table 4.8 The performance comparison with
Table Mountain-Tesla outage (COI transfer margin)

	Network 1	Network 2	Network 3	Network 4	Network 5	System
Max error (MW)	46.68	44.04	82.38	112.70	50.44	25.94
Mean error (MW)	11.53	10.02	14.39	38.94	11.00	5.63
Standard deviation (MW)	11.54	10.05	14.45	39.10	11.05	5.66

Table 4.9 The performance comparison with
Diablo Canyon unit outage (COI transfer margin)

	Network 1	Network 2	Network 3	Network 4	Network 5	System
Max error (MW)	37.81	59.84	66.83	42.24	33.17	28.60
Mean error (MW)	9.92	14.41	11.13	13.49	7.91	7.00
Standard deviation (MW)	10.00	14.51	11.10	13.39	7.98	7.05

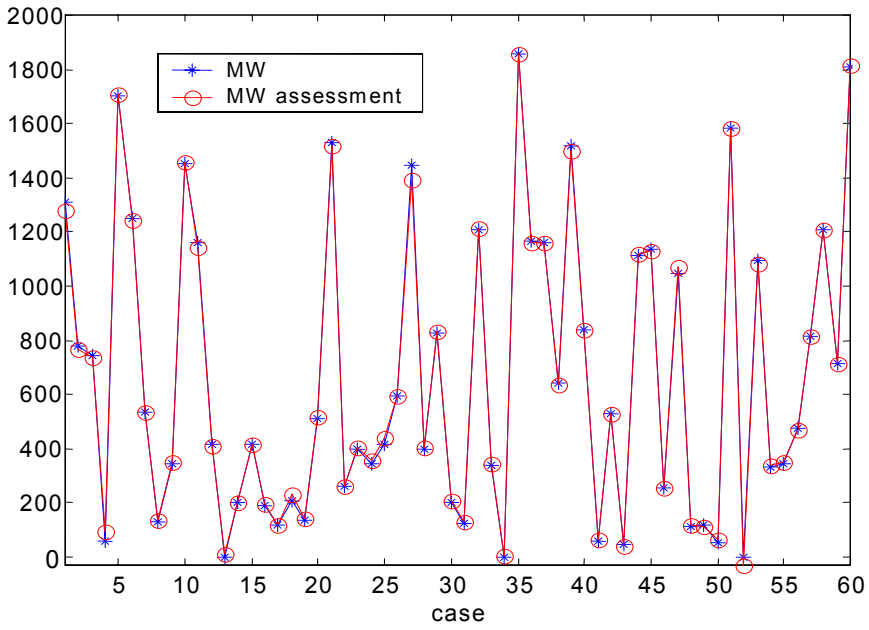

Figure 4.5 The performance of the system model including Table Mountain-Tesla outage (COI transfer margin)

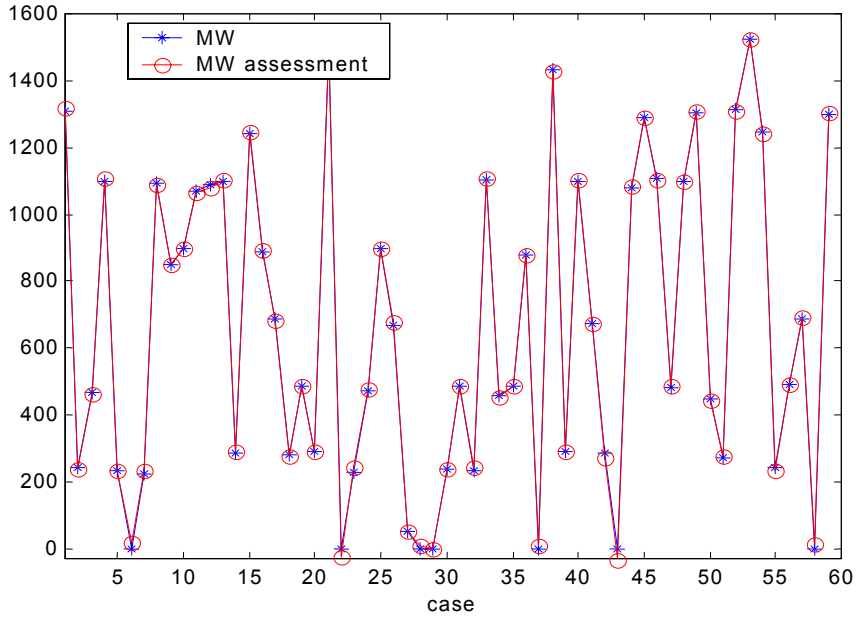

Figure 4.6 The performance of the system model including Diablo Canyon outage (COI transfer margin)

5. Conclusions

5.1 Remarks

This study investigates some approaches to improving operator procedures with particular emphasis on estimating transfers limited by voltage security using neural networks. In practice, the relations between critical paths and operating conditions are tabulated and plotted as nomograms for on-line use by system operators. With such a simplified view of system conditions, the operator is often unable to have a complete understanding of operational limits.

The neural network implicitly models the relation between security and the system loading and power flow patterns in the interested area. Here for VSA, static analysis methods, which are commonly used by utilities, are employed but there are no limitations to this in the proposed approach. Thus, a general methodology for fast on-line security assessment has been proposed. Two kinds of neural networks, Kohonen networks and feedforward neural networks, are investigated. The latter is found to be more suitable for this problem. Feature selection is based on both engineering knowledge and statistical correlation. Principle component analysis is used for further feature reduction and data preprocessing. For robustness, multiple networks are used with the final estimated based on an average after tossing out the lowest and highest estimations. Different system operating conditions (winter, summer), different loading levels and contingency plans are used for generating training and testing data. These different scenarios mimic the studies and methods used in utilities. The data comes from computations using mature algorithms developed for static security analysis. As was done in this study, it is straightforward to present the procedures with the estimated margins in a database. Therefore, the method can be easily embedded into the security analysis module in a modern energy management system. Excluding the training period, the neural networks operate extremely fast and are suitable for on-line application.

Specific contributions from this study were:

- A typical set of operating procedures was tabulated into an on-line database. Conceptually, these margins can be easily modified on-line to reflect changing system conditions.
- Several pattern matching type approaches were investigated using a modified New England 39 bus system. Based on these results, a system based on feedforward artificial neural networks (ANN) was designed.
- A modified ANN system, employing multiple networks and a voting system, was applied to the Western System Coordinating Council (WSCC) system. The analysis was based on a WSCC 5000 bus model over a large range of loading conditions considering all major contingencies.
- Results on P margin estimations for the California Oregon Intertie showed no misclassifications of security and an average error of 1.2%.
- Results on P margin estimations for the California area showed no misclassifications of security and average error of 3.7%.

- A single estimator covering select multiple contingencies raised margin errors on the California Oregon Intertie to 5.8% but again there were no misclassifications of security. Conceptually, this situation represents a flexible multivariate nomogram.

The test results shown here establish that using a system of feedforward ANNs, one can accurately estimate security margins for on-line application. In practice, the operating schedules face the possibility of numerous combinations of operating conditions and equipment outages. To avoid a proliferation of estimators, it is important that a single network can perform well under some multiple contingencies. The results show that some such combinations can be solved using only one set of neural networks. Thus, one may be able to provide a complete system assessment with a manageably small number of networks, each trained for a limited set of multiple outages.

Finally, the effectiveness of the method, of course, depends largely on the credibility of the data. That is, to what extent does the data used for training represent the unstudied cases? For the voltage security assessment problem studied here, this condition appears to be reasonable. There is a trade-off here between accuracy of the approach, number of networks and number of off-line studies. That is, this approach requires operation planners to increase somewhat the number of off-line studies, as well as carefully record data, so as to improve the estimates. Further, more accurate results are obtained if each estimator (set of networks) is limited to only one double contingency.

5.2 Further research

While the results presented in this work show the validity of the ANN approach, there are several extensions needed for practical on-line application. First, only one security problem has been investigated here. A practical system must consider all security criteria, including thermal limits, voltage decay, voltage dip, and so on. Second, greater use of on-line data may improve the performance significantly. For example, for the problem at hand, there is a well-known indication of voltage collapse: a small change in power flow causing large change in voltage. Measurements, where available, that indicate such a condition could also be features inputted into a neural network. Further, the objective is to use the system to not only calculate the margin but also to determine transfer limits based on the margin estimate and other security inputs.

Bibliography

[1] Colorado Coordinated Planning Group et. al. *Determination of available transfer capability within the western interconnection*. February 18, 1997

[2] Pacific Gas & Electric. *S5 procedures*, March, 1994

[3] IEEE Special Publication, 90TH0358-2-PWR, *Voltage Stability of Power Systems: Concepts, Analytical Tools and Industry Experience*, 1990

[4] Abbas Aded, et. al., *Proposed Voltage Stability Guidelines, Undervoltage Load Shedding Strategy, and Reactive Power Reserve Monitoring Methodology, Final Report*, Reactive Power Reserve Work Group, Technical Studies Subcommittee, Western System Coordinating Council, Sept. 1997.

[5] P. Kundur, *Power System Stability and Control,* McGraw-Hill, 1994, New York.

[6] Carson W Taylor, *Power System Voltage Stability*, McGraw-Hill, 1994, New York.

[7] A.J. Wood and B.F. Wollenberg, *Power Generation, Operation, and Control,* John Wiley & Sons, 1996

[8] B. Gao. G.K. Morison and P. Kundur, "Voltage stability evaluation using modal analysis," *IEEE Transactions on Power Systems,* Vol. 7, No.4, Nov. 1992, p1529-1542

[9] P.A. Lof, G. Anderson and D.J. Jill, "Voltage stability indices for stressed power system," *IEEE Transactions on Power Systems*, Vol. 8, No. 1, Feb. 1993, p 326-335

[10] C.A. Canizares, A.Z. de Souza and V.H. Quintana, "Comparison of performance indices for detection of proximity to voltage collapse*," IEEE Transactions on Power Systems,* Vol. 11, No. 3, Aug, 1996, p 1441-1450

[11] C.A. Canizares, F.L. Alvarado, C.L. DeMarco, I. Dobson and W.F. Long, "Point of collapse methods applied to ac/dc power systems," *IEEE Transactions on Power Systems,* Vol. 7, No. 2, May 1992, pp.673-683

[12] V. Ajjarapu and C. Christy, "The continuation power flow: A tool for steady state voltage stability analysis," *IEEE Transactions on Power Systems*, Vol. 7, No. 1, Feb. 1992, pp.416-423

[13] C.J. Parker, I.F. Morrison and D. Sutanto, "Application of an optimization method for determining the reactive margin from voltage collapse in reactive power planning," *IEEE Transactions on Power Systems*, Vol. 11, No. 3, Aug. 1996, pp.1473-1481

[14] G.C. Ejebe, G.D. Irisarri, S. Mokhtari, O. Obadina, P. Ristanovic and J. Tong, "Methods for contingency screening and ranking for voltage stability analysis of power system," *IEEE Transactions on Power Systems,* Vol. 11, No. 1, Feb. 1996, pp.350-356

[15] H.D. Chiang, C.S. Wang and A.J. Flueck, "Look-ahead voltage and load margin contingency selection functions for large-scale power systems," *IEEE Transactions on Power Systems*, Vol. 12, No. 1, Feb. 1997, pp.173-180

[16] S. Greene, I. Dobson and F.L. Alvarado, "Contingency ranking for voltage collapse via sensitivities from a single nose curve," *IEEE Transactions on Power Systems*, Vol. 14, No. 1, Feb. 1999, pp.232-238

[17] B. Avramovic, "On Neural Network Voltage Assessment," *Proceedings of INNS/EPRI Summer Workshop on Neural Networks Computing for the Electric Power Industry*, Stanford, CA, Aug. 1992.

[18] A. A. EI_Keib and X. Ma, "Application of Artificial Neural Networks in Voltage Stability Assessment," *IEEE Transactions on Power System*, Vol. 10, No.4, Nov. 1995, pp. 1890-1896.

[19] J.A. Momoh, L.G. Dias, and R.Adapa, “Investigation of Artificial Neural Networks for Voltage Stability Assessment,” *Proceedings of the IEEE International Conference on Systems, Man and Cybernetics,* Vancouver, BC, 1995, pp. 2188-2192.

[20] Y.H. Song, H. B. Wan and A. T. Johns, “Power System Voltage Stability Assessment Using a Self-organizing Neural Network Classifier, *IEE Conference Publication Proceedings of the 1996 4th International Conference on Power System Control and Management*, no. 421, April 1996 London, UK, pp. 171-175.

[21] M. La Scala, M. Trovato, F. Torelli, “Neural Network-based Method for Voltage Security Monitoring,” *IEEE Transactions on Power Systems,* vol 11, no. 3, Aug 1996, pp. 1332-1341.

[22] S. Chauhan and M.P. Dava, “Kohonen Neural Network Classifier for Voltage Collapse Margin Estimation,” *Electric Machines and Power Systems*, vol. 25, no. 6, July 1997, pp. 607-619.

[23] D. Popovic, D. Kukolj and F. Kulic, “Monitoring and Assessment of Voltage Stability margins Using Artificial Neural Networks with a Reduced Input Set,” *IEE Proceedings: Generation, Transmission and Distribution,* vol. 145, no. 4, July 1998, pp. 355-362.

[24] Simon Haykin, *Neural networks : a comprehensive foundation*, Prentice Hall, 1999, Upper Saddle River, N.J.

[25] Stent, G.S., 1973. “A Physiological mechanism for Hebb’s postulate of learning,” *Proceedings of the National Academy of Sciences*, USA, vol. 70, pp997-1001.

[26] T.Kohonen. “Self-organized formation of topologically correct feature maps.” *Biological Cybernetics*, 66:59-69, 1982

[27] T.Kohonen. *Self-organization and associate memory*. Springer-Verlag, London, 1984

[28] Y. Mansour, editor, Suggested techniques for voltage stability analysis," *technical report 93TH0620-5PWR*, IEEE/PES, 1993.

[29] N. D. Hatziargyriou and T. Van Cutsem, editors, "Indices predicting voltage collapse including dynamic phenomena," *Technical report TF 38-02-11,* CIGRE,1994.

[30] A. Berizzi, P. Finazzi, D. Dosi, P. Marannino, and S. Corsi, First and second order methods for voltage collapse assessment and security enhancement," *IEEE/PES PE-422-PWRS-0-01-1997, Winter Meeting*, New York, NY, February 1997.

[31] IEEE/PES Power System Stability Subcommittee Special Publication: *Voltage Stability Assessment Procedures and Guides (Draft)* April 1999

[32] S. Greene, I. Dobson, and F.L. Alvarado, Sensitivity of the loading margin to voltage collapse with respect to arbitrary parameters," *IEEE Transaction on Power Systems,* vol. 12, no. 1, February 1997, pp. 262-272.

[33] EPRI TR-101931, *Voltage Stability/Security Assessment and On-Line Control, Volume 1, Final Report,* Prepared by Ontario Hydro, April 1993.

[34] EPRI TR-102004, *Extended Transient-Midterm Stability Program (ETMSP), Volume 1, Final Report,* Prepared by Ontario Hydro, May 1994.

[35] T. VanCutsem, C.D. Vournas, “Voltage Stability Analysis in Transient and Midterm Time Scales*”, IEEE Transactions on Power System.* v11, 1996, pp146-154.

[36] Nahman, J.; Skokljev, I. Fuzzy logic and probability based real time contingency ranking. *International Journal of Electrical Power and Energy System.* v22 n3 2000 Elsevier Science Ltd Exeter Engl p 223-229

[37] Cote, James W.; Liu, Chen-Ching. Voltage security assessment using generalized operational planning knowledge. *IEEE Transactions on Power Systems.* v 8 n 1 Feb 1993 p 28-34

[38] Liu, Chih-Wen; Chang, Chen-Sung; Su, Mu-Chun. Neuro-fuzzy networks for voltage security monitoring based on synchronized phasor measurements. *IEEE Transactions on Power Systems.* v 13 n 2, May 1998, p 326-332

[39] Van Cutsem, T.; Wehenkel, L.; Pavella, M.; Hellbornn, B.; Goubln, M. Decision tree approaches to voltage security assessment. *IEE Proceedings, Part C: Generation, Transmission and Distribution* v 140 n 3 May 1993 p 189-198

[40] Hong, Y.-Y.; Yang, Y.-L. Expert system for enhancing voltage security/stability in power systems. *IEE Proceedings: Generation, Transmission and Distribution* v 146 n 4 1999 IEE Stevenage Engl p 349-354

[41] Su, Ching-Tzong; Lin, Chien-Tung. Voltage/reactive power control via fuzzy linear programming approach. *Cybernetics and Systems* v 30 n 3 Apr-May 1999 Taylor & Francis Ltd p 213-226

[42] Ramakrishna, G.; Rao, N.D. Adaptive neuro-fuzzy inference system for volt/var control in distribution systems. *Electric Power Systems Research* v 49 n 2 Mar 1 1999 Elsevier Science S.A. Lausanne Switzerland p 87-97

[43] Su, Ching-Tzong; Lin, Chien-Tung. New fuzzy control approach to voltage profile enhancement for power systems. *IEEE Transactions on Power Systems* v11 n3 Aug 1996 p 1654-1659

[44] Tso, S.K.; Zhu, T.X.; Zeng, Q.Y.; Lo, K.L. Fuzzy reasoning for knowledge-based assessment of dynamic voltage security. *IEE Proceedings Generation, Transmission and Distribution* v143 n2 Mar 1996 p 157-162

[45] Yabe, K.; Koda, J.; Yoshida, K.; Chiang, K.H.; Khedkar, P.S.; Leonard, D.J.; Miller, N.W.Conceptual designs of AI-based systems for local prediction of voltage collapse. *IEEE Transactions on Power Systems* v11 n1 Feb 1996 IEEE Piscataway NJ USA p 137-145

[46] Bell, K.R.W.; Daniels, A.R.; Dunn, R.W. Security-constrained reactive dispatch using fuzzy logic. *Proceedings of the Universities Power Engineering Conference Proceedings of the 1995 30th Universities Power Engineering Conference*. 1995 v1 p61-64

[47] Levitin, G.; Mazal-Tov, S.; Reshef, B. Genetic algorithm for optimal planning of transmission system reactive power compensation under security constraints. *Proceedings of the Mediterranean Electrotechnical Conference - MELECON Proceedings of the 1998 9th Mediterranean Electrotechnical Conference*, p 897-900

[48] Wehenkel, L.; Van Cutsem, T.; Pavella, M.; Jacquemart, Y.; Heilbronn, B.; Pruvot, P. Machine learning, neural networks and statistical pattern recognition for voltage security: A comparative study. *International Journal of Engineering Intelligent Systems for Electrical Engineering and Communications* v2 n4 Dec 1994 p 233-245

[49] Maiorano, A.; Trovato, M. Neural network-based tool for preventive control of voltage stability in multi-area power systems : *Neurocomputing* v 23 n 1-3 Dec 1998 Elsevier Sci B.V. Amsterdam Netherlands p 161-176

[50] Chen, Y.-L. Weak bus oriented reactive power planning for system *security IEE Proceedings Generation, Transmission and Distribution* v 143 n 6 Nov 1996 p 541-545

[51] Yokoyama, Ryuichi; Niimura, Takahide; Nakanishi, Yosuke. Coordinated control of voltage and reactive power by heuristic modeling and approximate reasoning. *IEEE Transactions on Power Systems* v 8 n 2 May 1993 p 636-642

[52] Li, F.; Peh, C.H.; Dunn, R. Genetic algorithms based approach to combined active and reactive power dispatch. *Proceedings of the Universities Power Engineering Conference Proceedings of the 1998 33rd Universities Power Engineering Conference* - UPEC '98 Sep 8-Sep 10 1998 v1 1998 Edinburgh, p 375-378

[53] Howard Demuth and Mark Beale, "Neural Network Toolbox, For Use with MATLAB®," *User's Guide*, Ver 3.0", July 1997.

[54] Western Systems Coordinating Council, *Western Systems Coordinating Council Disturbance Report for the Power System Outage that Occurred on the Western*

Interconnection, August 10, 1996 1548 PAST. Approved by the WSCC Operations Committee on October 18, 1996

[55] Western Systems Coordinating Council, *Western Systems Coordinating Council Disturbance Report for the Power System Outage that Occurred on the Western Interconnection on-, July 2,1996 1424 PAST, July 3, 1996 1403 PAST*. Approved by the WSCC Operations Committee on September 19, 1996

[56] MacKay, D. J. C., "Bayesian interpolation," *Neural Computatio*n, vol. 4, no. 3, pp. 415-447, 1992.

[57] Amari, S., N. Murata, K.-R. Muller, M. Finke, and H. Yang, 1996a. "Statistical theory of overtraining-Is cross-validation asymptotically effective*?" Advances in Neural Information Processing Systems*, vol. 8, pp176-182, Cambridge, MA: MIT Press.

Project Research Products

Related Reports

L. Chen, *Neural Network Approaches for Estimating Margins in Power System Voltage Security Analysis*, MSEE Thesis, Washington State University, Pullman, WA, 2000.

L. Chen, K. Tomsovic, A. Bose and R. Stuart, "Estimating Reactive Margin for Determining Transfer Limits," *Proceedings of the 2000 IEEE PES Summer Meeting*, Seattle, July 2000.

L. Chen, K. Tomsovic, A. Bose and R. Stuart, "Estimating Power Transfer Margins for Voltage Security," submitted to *IEEE Transactions on Power Systems*.

Prototype software (available from K. Tomsovic)

Database implementation of S-5 operating procedures

Margin estimator for studied cases